

ChemComm

Chemical Communications

Accepted Manuscript

This article can be cited before page numbers have been issued, to do this please use: P. Meher, K. R. Thombare, S. Chandra and S. Murarka, *Chem. Commun.*, 2025, DOI: 10.1039/D5CC02800K.



This is an Accepted Manuscript, which has been through the Royal Society of Chemistry peer review process and has been accepted for publication.

Accepted Manuscripts are published online shortly after acceptance, before technical editing, formatting and proof reading. Using this free service, authors can make their results available to the community, in citable form, before we publish the edited article. We will replace this Accepted Manuscript with the edited and formatted Advance Article as soon as it is available.

You can find more information about Accepted Manuscripts in the [Information for Authors](#).

Please note that technical editing may introduce minor changes to the text and/or graphics, which may alter content. The journal's standard [Terms & Conditions](#) and the [Ethical guidelines](#) still apply. In no event shall the Royal Society of Chemistry be held responsible for any errors or omissions in this Accepted Manuscript or any consequences arising from the use of any information it contains.

FEATURE ARTICLE

Visible Light-Driven Chemistry of Diaryliodonium Reagents: Mechanistic Perspectives and Synthetic Applications

Prahallad Meher,^a Karan Ramdas Thombare,^a Sneha Chandra,^a and Sandip Murarka^{*a}Received 00th January 20xx,
Accepted 00th January 20xx

DOI: 10.1039/x0xx00000x

Diaryliodonium reagents (DAIRs) are highly electrophilic arylating agents widely utilized in organic synthesis, excelling in both metal-free and metal-catalyzed transformations. However, their reactivity and application as aryl radical precursors under visible-light irradiation remain relatively underexplored. Due to their easy availability, intrinsic reactivity, stability, and environmentally benign nature, they are promising candidates to serve as aryl radical surrogates in various visible light-induced synthetic transformations. In this feature article, we have reviewed our recent findings alongside other significant reports on the utility of DAIRs under visible light irradiation. We have discussed the diverse reactivity of DAIRs in a palette of visible light-mediated reactions leading to the construction of carbon-carbon or carbon-heteroatom bonds. In addition, their role as atom transfer agents, including hydrogen atom transfer (HAT) and halogen atom transfer (XAT), has also been discussed.

Introduction

Diaryliodonium reagents (DAIRs) have received significant attention as electrophilic aryl transfer agents during the last decade due to their environmental friendliness, stability, high reactivity, and appreciable selectivity.¹ They are typically represented as T-shaped molecules, where the counterion shares a three-centre four-electron bond with the iodine and the apical aryl group.^{1b} Classified as hypervalent iodine (III) reagents, DAIRs have found broad applications in both metal-free and metal-catalyzed reactions, enabling the formation of carbon-carbon and carbon-heteroatom bonds with remarkable efficiency.² These reactions primarily proceed through an ionic pathway where DAIRs can be regarded as a surrogate of aryl cation. Notably, non-photoinduced metal-free arylations involving DAIRs have also been reported to operate via a single-electron transfer (SET) mechanism.^{2f, 3}

Recently, there has been an upsurge in the literature concerning the reactivity of DAIRs as an aryl radical precursor under visible light irradiation. Aryl radicals are highly reactive intermediates that can react with a variety of functional groups to provide value-added products.⁴ Their high reactivity provides an alternative reaction paradigm to conventional polar counterparts. However, aryl radicals are more reactive than Csp³ radicals; hence, controlling their formation and subsequent reactivity often imposes considerable challenges.^{4c} Traditionally, aryl radicals are generated through various methods, including the thermal decomposition of diaryl peroxides, the reaction of suitable aromatic precursors with stoichiometric oxidants or reductants, or by exposing aryl radical precursors to high-energy UV light.^{4c} The radical

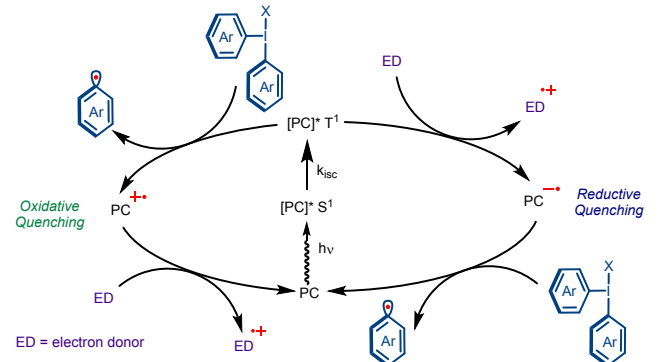
generation through direct photoexcitation with high-energy UV light renders the synthetic processes uncontrolled, unselective, and synthetically less desirable. Hence, the generation of high-energy reactive radicals, such as aryl radicals, in a selective manner under mild conditions is at the forefront of modern organic synthesis. In this regard, visible light-induced synthetic transformations provide a mild and sustainable tool for generating aryl radicals, thereby dramatically expanding the potential of synthetic strategies that leverage such reactive radicals.⁵ Among the most popular substrates are aryl diazonium salts, aryl sulfonyl chlorides, aryl halides, and aryl sulfonium salts, which can produce aryl radicals under the irradiation of visible light and have been reviewed elsewhere.⁴ This feature article instead focuses on the emergence of DAIRs as easy-to-prepare, bench-stable, and synthetically useful aryl radical surrogates, furnishing a multitude of reactivity under visible light irradiation.

In general, the reduction potential of DAIRs ranges from approximately -0.1 to -0.8 V vs. SCE in acetonitrile, depending on their electronic and structural features,⁶ which is well within the reach of the excited-state redox potentials of commonly used photocatalysts, such as [Ru(bpy)₃]^{III/II*} ($E_{1/2}^* \approx -0.81$ V vs. SCE), [fac-Ir(ppy)₃]^{IV/III*} ($E_{1/2}^* \approx -1.73$ V vs. SCE), [eosin Y]^{•+/•} ($E_{1/2}^* \approx -1.11$ V vs. SCE) under photochemical conditions.^{5d, 7} This thermodynamic match supports the feasibility of a photoinduced SET pathway leading to aryl radical generation. Mechanistically, DAIRs could lead to the generation of aryl radicals under visible light-driven single-electron transfer (SET) processes in the presence or absence of an exogenous photocatalyst. Photocatalysis involves photoexcitation of an external light-harvesting molecule (photocatalyst)- an organic dye or metal complex, which in its excited state becomes a strong single-electron reductant or oxidant (Scheme 1A).^{5b, 5c} Subsequently, the excited photocatalyst engages in SET

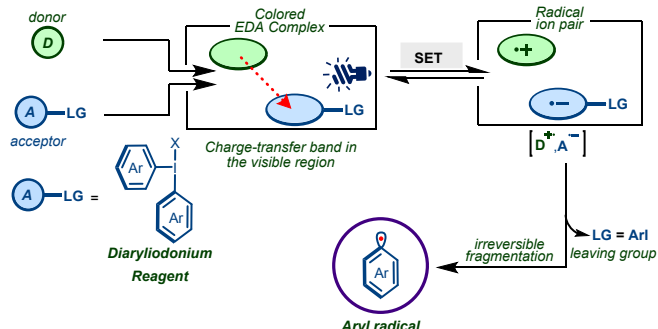
^a Department of Chemistry, Indian Institute of Technology Jodhpur, Karwar-342037, Rajasthan, India. Email: sandipmurarka@iitj.ac.in.

processes with another molecule leading to the formation of an aryl radical. Alternatively, in the absence of a photocatalyst, DAIRs can form an electron donor-acceptor (EDA) complex with an electron-rich donor molecule in the ground state (Scheme 1B). This complex is characterized by a distinct charge transfer band that absorbs light typically in the visible region, and light irradiation at this wavelength triggers the SET event, producing a radical ion pair.⁸ Finally, radical anion species, upon fast and irreversible fragmentation, form aryl radicals, primed to indulge in diverse reactivity, and aryl iodide leaves as the leaving group. Notably, on most occasions, the aryl iodide byproduct can be recovered and efficiently recycled, rendering the process economically viable.

A. Photoredox catalyzed reactions



B. EDA Complex Formation



Scheme 1 General reactivity of diaryliodonium reagents under visible light irradiation

The design of productive photoinduced transformations using DAIRs hinges on several factors. Crucial among these is the redox potential match between DAIRs and the photocatalyst, which governs SET feasibility, along with the light absorption properties and excited-state lifetimes of the photocatalyst^{5c} or EDA complex^{8e} to ensure efficient photoexcitation and minimize quenching. The stability and reactivity of radical intermediates are key to achieving selective transformations, while substrate electronics and sterics shape the rate and regioselectivity of radical trapping.⁹ Furthermore, solvent, base, concentration, and oxygen sensitivity play crucial roles related to reactivity. Finally, practical aspects such as light source compatibility, photon flux, and scalability are essential for efficient and applicable processes. Importantly, the counterion in DAIRs critically influences reaction outcomes. Non-coordinating anions like BF_4^- , PF_6^- , OTf^- , and OTs^- improve solubility in organic solvents and ensure homogeneous conditions. They

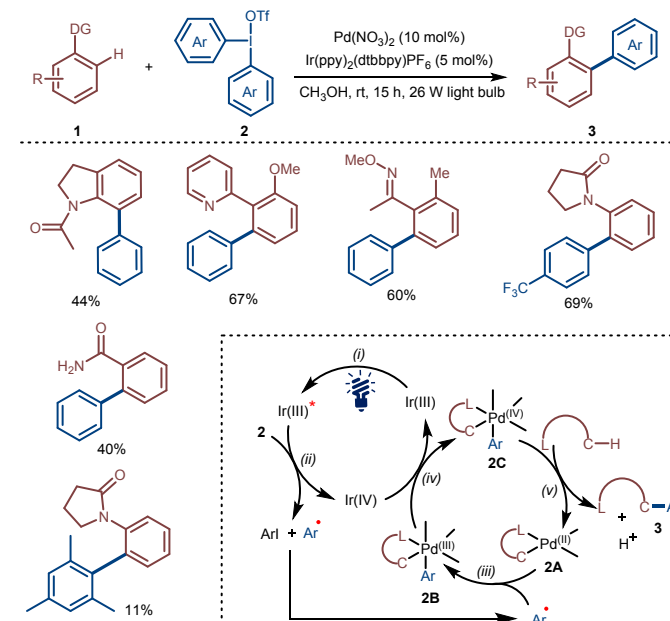
also modulate the iodine(III) centre's electrophilicity, affecting the rate and efficiency of aryl radical generation during SET processes. This feature article intends to summarize our contributions in the area of visible light-induced synthetic transformations involving DAIRs while covering related contemporary discoveries from other groups. We begin by highlighting two-component and multicomponent photoinduced arylation strategies involving DAIRs and then move on to discuss more contemporary concepts involving hydrogen atom transfer (HAT)¹⁰ and halogen atom transfer (XAT)¹¹ processes. For a better understanding of the readers, the photoinduced arylation part is further categorized according to the type of bond formation, covering the mechanistic aspects.

1. Two-Component Reactions

In this section, we have discussed the photogeneration of aryl radicals from DAIRs by photoredox catalysis or EDA complexes and a variety of two-component reactions they undergo. We spotlight important C-C and C-X bond-forming strategies covering the mechanistic aspects of aryl radical generation and subsequent steps.

1.1 Photoredox Catalysis

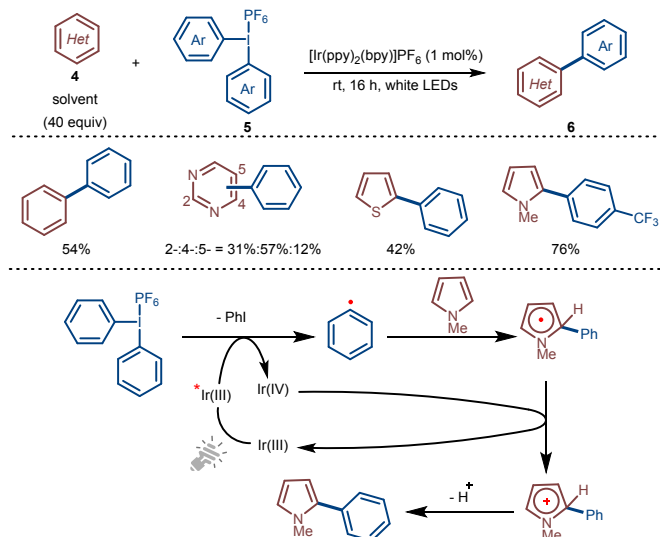
1.1.1 Csp²—Csp² Bond Formation



Scheme 2 Pd/Ir dual photoredox-catalyzed directed C-H arylation of arenes

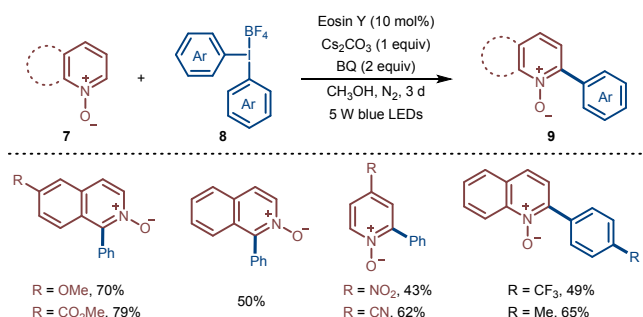
Direct Csp²-H functionalization of heterocycles has attracted significant attention due to its importance in pharmaceuticals and drug discovery.¹² Even small modifications to these structures can profoundly influence their bioactive profiles. Among the various applications, aryl-aryl cross-coupling stands out as one of the most widely studied topics in the synthesis of value-added products. In 2012, the Sanford group reported a photoredox palladium/iridium-catalyzed directed Csp²-H arylation of various arenes **1** using DAIRs as an aryl radical source (Scheme 2).¹³ In contrast to the traditional transition metal-catalyzed C-H activation reactions proceeding

through the ionic 2e pathway at high temperature, this reaction operated via a radical mechanism at room temperature. According to the proposed mechanism, the reaction begins with photoexcitation of Ir³⁺ to Ir^{3+*}, which reduces DAIRs **2** to generate Ir⁴⁺, aryl radical, and aryl iodide. The resulting aryl radical subsequently oxidizes cyclopalladated complex **2A** to **2B**, which further gets oxidized by Ir⁴⁺ to produce **2C**, while completing the photocatalytic cycle. Finally, reductive elimination from complex **2C** delivers final arylated arenes **3**.



Scheme 3 Csp²-H arylation of (hetero)arenes via Ir-photoredox catalysis

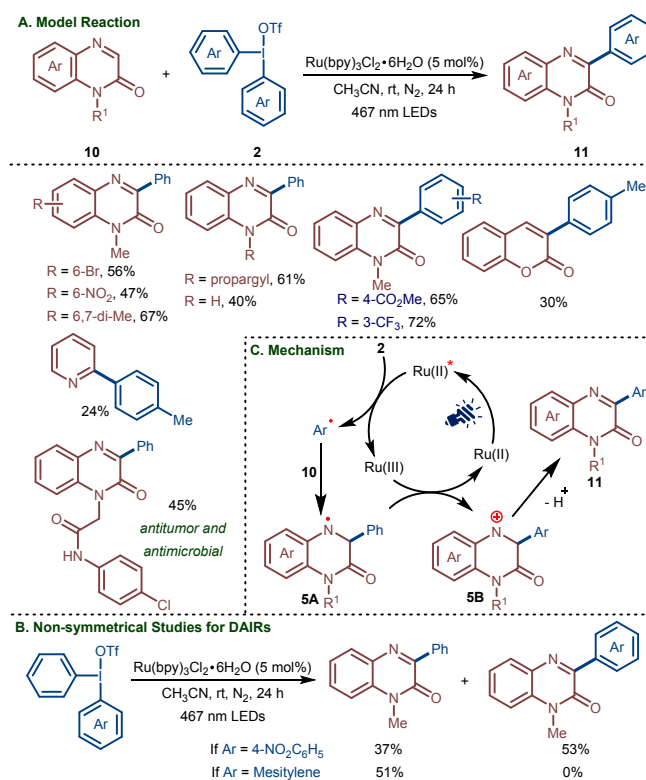
Subsequently, Chatani and co-workers further expanded the application of DAIRs under photoredox catalysis by documenting an iridium-catalyzed arylation of benzene and heteroarenes **4** such as pyridine, thiophene, and pyrrole (Scheme 3).¹⁴ The method exhibited a broad scope, providing corresponding arylated heteroarenes **6** in moderate to good yields. Mechanistically, the excited photocatalyst undergoes oxidative quenching by diphenyliodonium salt to generate phenyl radical, which, upon interaction with heterocycles, such as pyrrole, through a cascade of events comprising addition/oxidation/deprotonation, furnishes the final product. Along this line, Song, Gao, and co-workers discovered a C-2 selective arylation of quinoline and pyridine N-oxides **7** using DAIRs **8** under organophotoredox-catalyzed conditions (Scheme 4).¹⁵ The reaction exhibited broad scope with good functional group tolerance and provided access to a variety of 2-aryl-substituted quinoline and pyridine N-oxides **9** under operationally simple conditions.



Scheme 4 C-2 selective Csp²-H arylation of quinoline and pyridine N-oxides

DOI: 10.1039/D5CC02800K

In 2022, Murarka and co-workers developed a Ru-photoredox-catalyzed direct Csp²-H arylation of quinoxaline-2(1H)-ones **10** using diaryliodonium reagents **2** under mild and practical conditions (Scheme 5A).¹⁶ A palette of electronically and structurally diverse DAIRs **2** reacted with **10** to provide corresponding products **11** in moderate to excellent yields. Interestingly, the method enabled synthesis of quinoxalinone-based biologically active compounds and was successfully extended to the arylation of other heterocycles, such as coumarin and pyridine. Notably, evaluation of non-symmetrical DAIRs revealed that transfer of an electron-deficient and less sterically encumbered aryl ring was preferred (Scheme 5B). The proposed mechanism, supported by detailed mechanistic investigations, involves the reduction of DAIRs by the excited Ru(II)* photocatalyst to generate Ru(III) and aryl radical, which then undergoes selective addition at the C-3 position of quinoxaline-2(1H)-one (Scheme 5C). Finally, oxidation of radical intermediate **5A** by Ru(III) followed by deprotonation affords arylated quinoxaline-2(1H)-ones **11** and completes the photocatalytic cycle. Thereafter, a protocol for the selective arylation of 2-imino-2H-chromene-3-carbonitriles and decarboxylative *ipso*-arylation of 2-oxo-2H-chromene-3-carboxylic acids using DAIRs was also developed under similar Ru-photocatalytic conditions.¹⁷

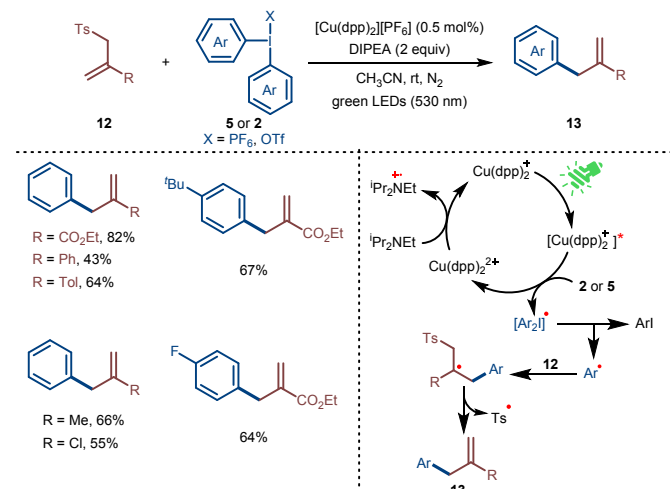


Scheme 5 Direct Csp²-H arylation of quinoxaline-2(1H)-ones via Ru-photoredox catalysis

1.1.2 Csp²–Csp³ Bond Formation

Selective functionalization of sp³-carbons under mild reaction conditions remains a highly intriguing area in organic synthesis, as many drugs and pharmaceuticals contain Csp³ centers. However,

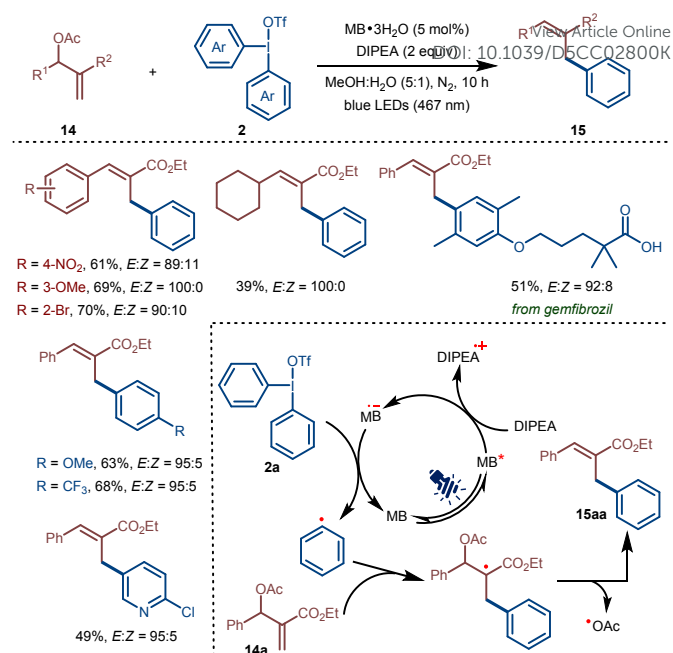
incorporating an arene ring on the Csp³ backbone through a site-selective Csp³–Csp² coupling is far from being trivial. Recently, visible light photochemical reactions have emerged as a promising platform for achieving selective functionalization of sp³-carbons.¹⁸



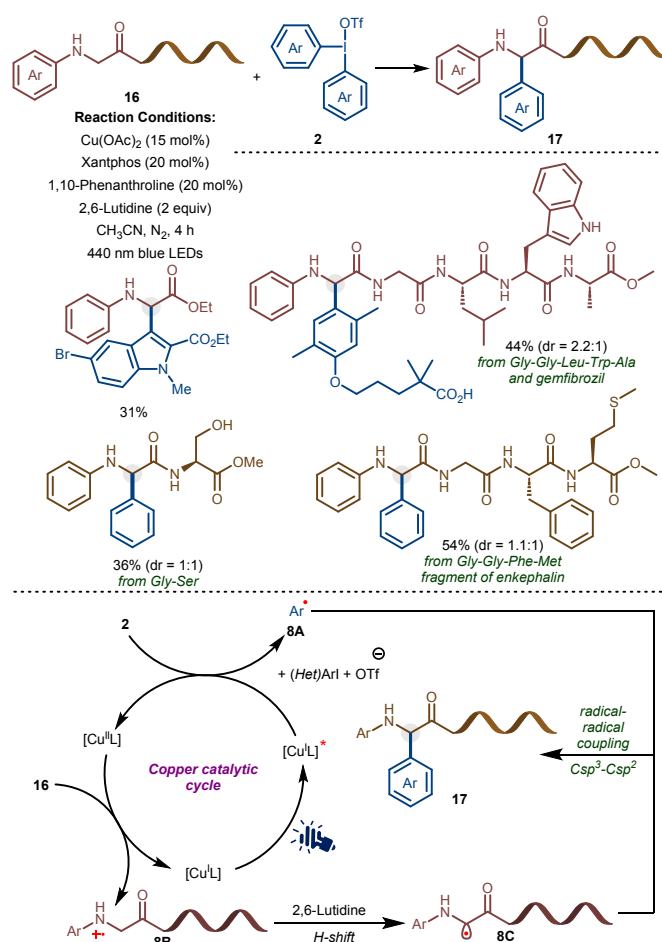
Scheme 6 Copper-photoredox catalyzed allylic arylation of allyl sulfones

The allylation reaction holds significant importance in organic synthesis due to the ease of manipulation of the introduced allyl group into a variety of functional groups.¹⁹ In 2013, the Ollivier group introduced a copper-based photocatalytic protocol for the generation of aryl radicals from DAIRs as an alternative to Ru and Ir-photocatalysis (Scheme 6).²⁰ Notably, the aryl radical generated under copper-photoredox-catalyzed conditions was tamed for the allylic arylation of allyl sulfones **12** under mild conditions. In general, the base metal photocatalytic conditions enabled access to various allylated products in good yields. The authors proposed that [Cu(dpp)₂]⁺ initially gets excited upon irradiation with green LED and subsequently undergoes oxidative quenching with DAIRs to form [Cu(dpp)₂]²⁺, aryl iodide, and an aryl radical. Subsequently, the aryl radical reacts with allyl sulfones **12** to furnish the final products **13**. Meanwhile, the Cu(I) catalyst is regenerated through the reduction of [Cu(dpp)₂]²⁺ by *N,N*-diisopropylethylamine (DIPEA).

In 2024, the Murarka group developed a novel method for the arylation of Morita-Baylis-Hillman (MBH) acetates **14** using DAIRs **2** under organo-photoredox conditions to provide corresponding trisubstituted alkenes **15** in moderate to good yields (Scheme 7).²¹ The method worked well with a variety of aryl, heteroaryl, and aliphatic aldehyde-derived MBH acetates **14**, and various electronically and structurally diverse DAIRs **2**. A broad scope with good functional group tolerance, mild reaction conditions, and suitability for late-stage modification of drug molecules are some of the salient features of this method. The proposed mechanism involves reductive quenching of the excited organo-photocatalyst (MB*) by DIPEA, generating highly reductive photocatalyst MB^{•−}, which then engages with diphenyliodonium triflate **2a** (DPIT) by a SET process to produce phenyl radical while regenerating the photocatalyst. A subsequent S_N2'-type substitution on MBH acetate **14a** by phenyl radical delivers the final product **15aa**.



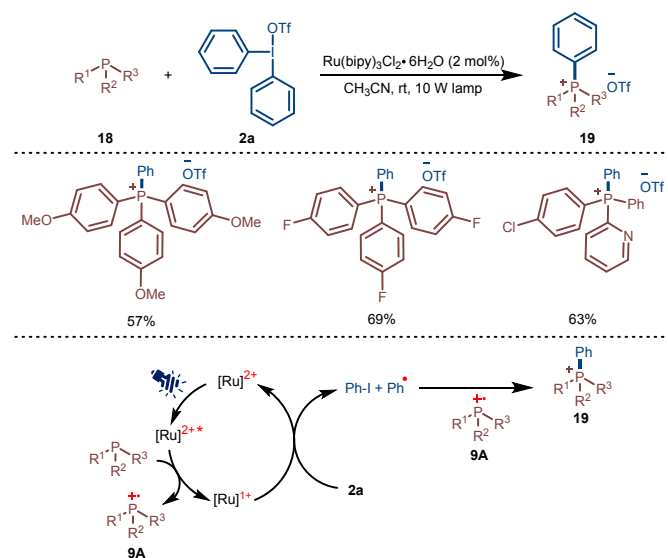
Scheme 7 Organo-photoredox catalyzed arylation of MBH acetates using diaryliodonium reagents



Scheme 8 Site-selective Csp³-H arylation of glycines and peptides under copper-photoredox catalysis

Unnatural amino acids exhibit unique and exceptional chemical properties as compared to natural amino acids, making them invaluable in advancing organic synthesis and drug discovery.²² Notably, α -arylglycines possess remarkable biological activity and serve as critical building blocks in many pharmaceuticals.²³ In this context, Murarka and co-workers developed an innovative approach for the site-selective Csp³-H arylation of glycines and peptides under copper-photoredox conditions (Scheme 8).²⁴ It is important to mention that this was one of the first reports on utilizing DAIRs as arylating reagents under photoinduced base-metal-catalyzed conditions. The method was successfully applied to the cross-coupling of a palette of electronically and structurally diverse DAIRs with glycine derivatives, providing a plethora of arylated glycine derivatives in good yields. The method was applicable to site-selective (hetero)arylation of short-chain and long-chain peptides and enabled peptide drug bioconjugation. Based on extensive mechanistic studies, it was proposed that the reaction begins with the photoexcitation of the copper(I) complex to generate [Cu(I)L]*, which then involves DAIRs through a SET process to produce aryl radical **8A** and [Cu(II)L] complex. The Cu(II) species returns to its original state by accepting an electron from glycine derivative **16**, which, in the presence of a base, generates the corresponding α -amino carbon radical **8C**. Finally, persistent radical effect-driven radical-radical cross-coupling between Csp³-radical **8C** and Csp²-radical **8A** leads to the formation of site-selective arylated products **17**.

1.1.3 Csp²-P Bond Formation



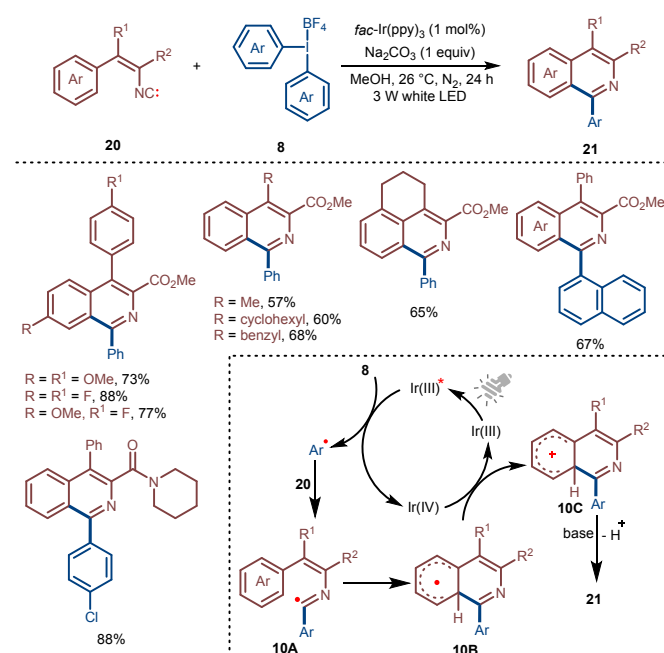
Scheme 9 Synthesis of quaternary arylphosphonium salts via Ru-photoredox catalysis

The formation of carbon-carbon bonds is the backbone of organic synthesis, but the creation of carbon-heteroatom bonds is equally fundamental due to their prevalence in numerous pharmaceuticals, drugs, and natural products.²⁵ In 2016, Denton and co-workers developed a Ru-photoredox-catalyzed synthesis of quaternary aryl phosphonium salts **19** in moderate to good yields using DPIT **2a** as a phenyl group surrogate (Scheme 9).²⁶ The method facilitated the forging of carbon-phosphorus bonds in a regioselective manner at ambient temperature. The authors proposed that initially,

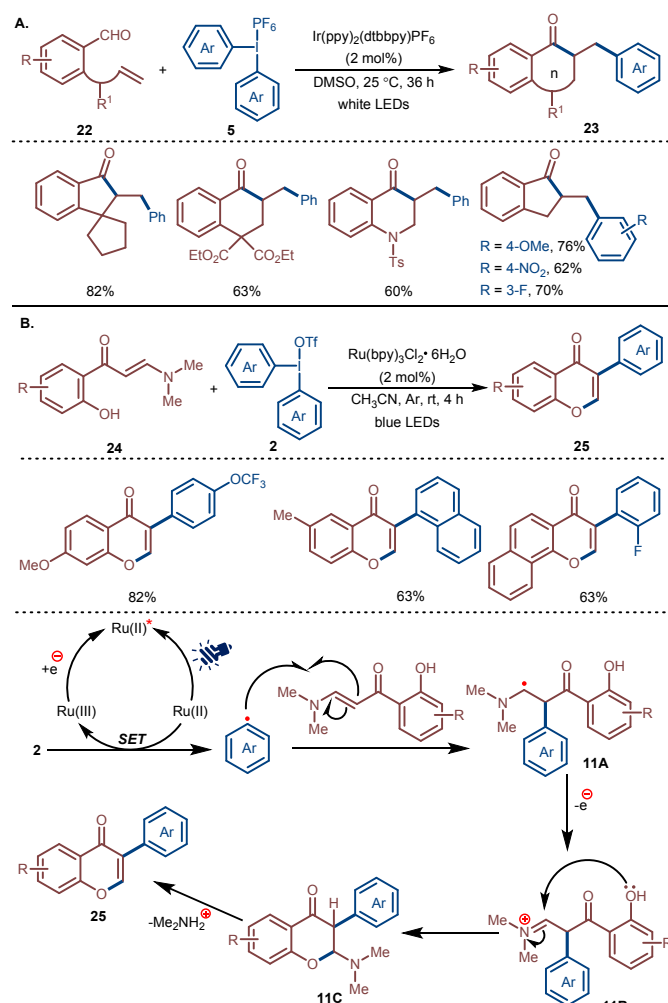
the excited Ru-photocatalyst gets reductively quenched by phosphines **18**, forming the phosphonium radical cation **9A** and Ru(I) species. Subsequent reduction of DPIT **2a** by the Ru(I) species produces a phenyl radical and iodobenzene, thereby completing the catalytic cycle (Scheme 9). The final aryl phosphonium salt **19** could be formed by direct coupling of the phosphoniumyl radical cation **9A** with the phenyl radical. Based on the control experiments, this pathway was proposed as the major pathway. However, the possibility of a photo-catalyst-free charge-transfer pathway and radical chain mechanism was not ruled out.

1.1.4 Cascade Annulation

Cascade annulation is a powerful and straightforward approach for synthesizing structurally diverse heterocycles that form the backbone of many biologically active compounds and pharmaceuticals. In 2014, Yu and co-workers developed a cascade annulation strategy for synthesizing highly substituted isoquinoline derivatives **21** in good yields (Scheme 10).²⁷ The redox-neutral method employed vinyl isocyanides **20** and DAIRs **8** as coupling partners under Ir-photoredox-catalyzed conditions, proceeding via a homolytic aromatic substitution (HAS) pathway. While several symmetrical DAIRs participated in the process, in the case of unsymmetrical ones, a preference for the electron-deficient aryl ring was observed. The reaction begins with the photoexcitation of the Ir(III) catalyst by white LED, followed by oxidative quenching of the excited catalyst with DAIRs **8** to generate an aryl radical. Subsequently, the aryl radical inserts into the vinyl isocyanide **20**, forming an imidoyl radical intermediate **10A**. The radical intermediate **10A** undergoes intramolecular HAS to provide intermediate **10B**, which, upon oxidation by Ir(IV), forms cationic intermediate **10C** along with the regeneration of the Ir(III) catalyst. Finally, deprotonation of the cationic intermediate by sodium carbonate yields isoquinoline derivatives **21** as the final product.

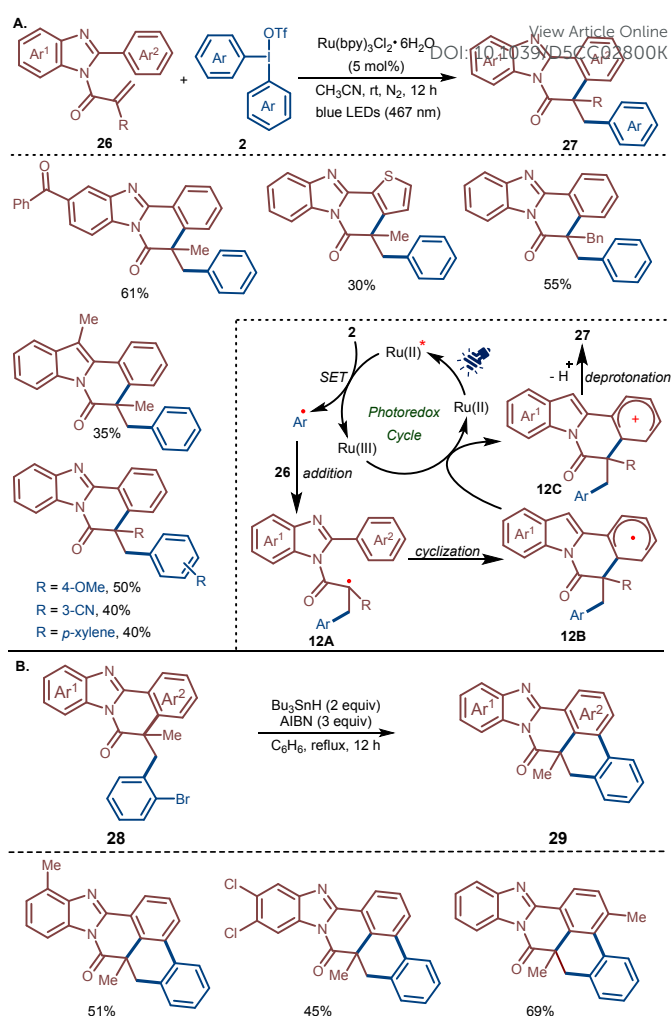


Scheme 10 Synthesis of isoquinolines via insertion of vinyl isocyanides with diaryliodonium reagents



Scheme 11 Visible light-mediated cascade annulation strategy for the synthesis of fused cyclic molecules

In 2018, Zhu and co-workers introduced an Ir-photoredox-catalyzed acylarylation of unactivated alkenes **22** with DAIRs **5**, leading to the synthesis of various heterocycles **23**, including 2-benzyl indanones, 3,4-dihydronaphthalen-1(2H)-ones, and 2,3-dihydroquinolin-4(1H)-ones in moderate to good yields (Scheme 11A).²⁸ The method featured a broad substrate scope, excellent diastereoselectivity, and mild reaction conditions. Subsequently, Laroshenko and co-workers developed a Ru-photoredox-catalyzed synthetic approach to access isoflavones **25** by reacting *ortho*-hydroxyarylenaminones **24** with DAIRs **2** (Scheme 11B).²⁹ Notably, several DAIRs **2** embedded with diverse functional groups underwent facile transformation to provide a variety of 3-aryl substituted chromones in moderate to good yields. The reaction proceeds through the addition of the *in situ* generated aryl radicals from DAIRs **2** under photocatalyzed conditions on the enaminones **24** to provide radical intermediate **11A**, which, upon oxidation with concomitant domino cyclization, forms the pyrone ring framework **11C**. Finally, the elimination of dimethylamine from intermediate **11C** delivers the desired chromones **25**.

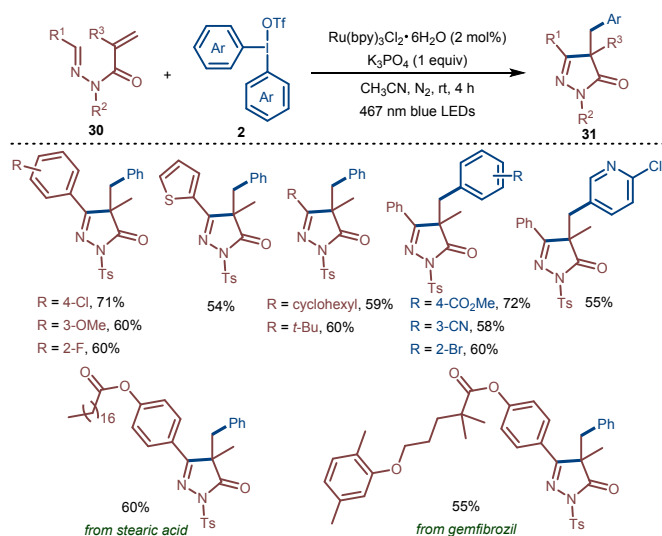


Scheme 12 Synthesis of benzimidazo[2,1-*a*]isoquinolin-6(5H)-ones

Lately, the Murarka group reported a Ru-photoredox catalyzed arylative radical cascade involving *N*-acryloyl-2-arylbenzimidazoles **26** and DAIRs **2** for the facile synthesis of biologically relevant arylated benzimidazo[2,1-*a*]isoquinolin-6(5H)-one derivatives **27** (Scheme 12A).³⁰ The reactions were carried out under amenable conditions, and the method demonstrated scalability and a broad scope with regard to both the reacting partners. Along the expected lines, the detailed study with unsymmetrical DAIRs revealed that under photoredox-catalyzed conditions, the transfer of electron-deficient and sterically less hindered aryl rings was preferred. Based on exhaustive mechanistic studies comprising radical trapping experiments and photophysical studies, the authors established the intermediacy of aryl radicals and ruled out the possibility of a radical chain mechanism. It was proposed that initially, the excited Ru(II) photocatalyst undergoes oxidative quenching by DAIRs **2** to generate Ru(III) catalyst, aryl iodide, and aryl radical. Afterward, the aryl radical adds to *N*-acryloyl-2-arylbenzimidazole **26**, forming a stable tertiary alkyl radical intermediate **12A**, which then undergoes intramolecular radical cyclization with the neighboring aryl ring to generate intermediate **12B**. Finally, oxidation of intermediate **12B** by Ru(III) with concomitant deprotonation delivers the desired product **27**. Importantly, the final products were amenable to further synthetic manipulations and an increase in molecular complexity. For

instance, 2-arylated benzimidazoisoquinolinones **28** embedded with a bromine functionality at the *ortho*-position of the phenyl moiety underwent intramolecular homolytic aromatic substitution (HAS) to furnish highly fused polycyclic heterocycles **29** in moderate to good yields (Scheme 12B).

More recently, the same group disclosed a conceptually innovative approach to access biologically relevant functionalized pyrazolones **31** (Scheme 13).³¹ They documented a Ru-photoredox-catalyzed arylative radical cascade involving *N'*-arylidene-*N*-acryloylhydrazides **30** and DAIRs **2** to provide arylated pyrazolone derivatives **31** in moderate to good yields (Scheme 13). This approach featured a novel skeleton **30** with multiple diversifiable points as an aryl radical acceptor, which is appropriate for the synthesis of a library of closely related analogues. In general, the method demonstrated broad functional group compatibility and proved effective for late-stage modifications of various drug molecules and pharmaceuticals.

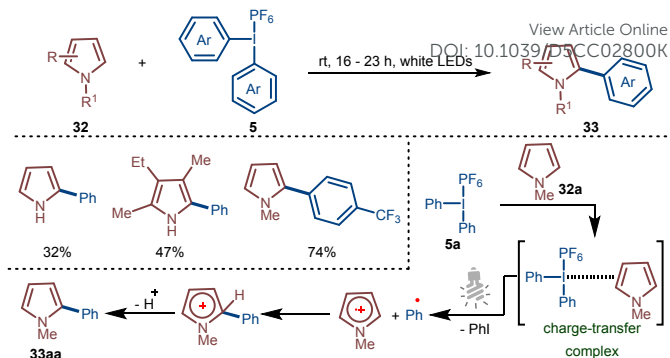


Scheme 13 Synthesis of pyrazolones *via* cascade annulation

1.2 EDA Complexes

1.2.1 Csp²–Csp² Bond Formation

The 2013 report by Chatani and co-workers on the Ir-catalyzed arylation of heteroarenes also featured the arylation of pyrroles **32** proceeding through EDA complex formation without any need for an exogenous photocatalyst (Scheme 14).¹⁴ Mechanistically, the EDA complex formed between pyrroles **32** and DAIRs **5** undergoes photoexcitation upon irradiation with white LEDs, initiating a SET from pyrrole **32a** to diphenyliodonium salt **5a** to produce a phenyl radical and iodobenzene as the by-product. Then, the phenyl radical undergoes addition to the C2 position of pyrrole **32a**, resulting in a cationic intermediate, which, upon subsequent deprotonation, furnishes phenylated pyrrole **33aa** as the final product. In general, sluggish reactivity was observed with electron-rich DAIRs in the photoarylation of pyrroles under EDA conditions, likely due to the ineffective formation of the charge transfer (CT) complex.



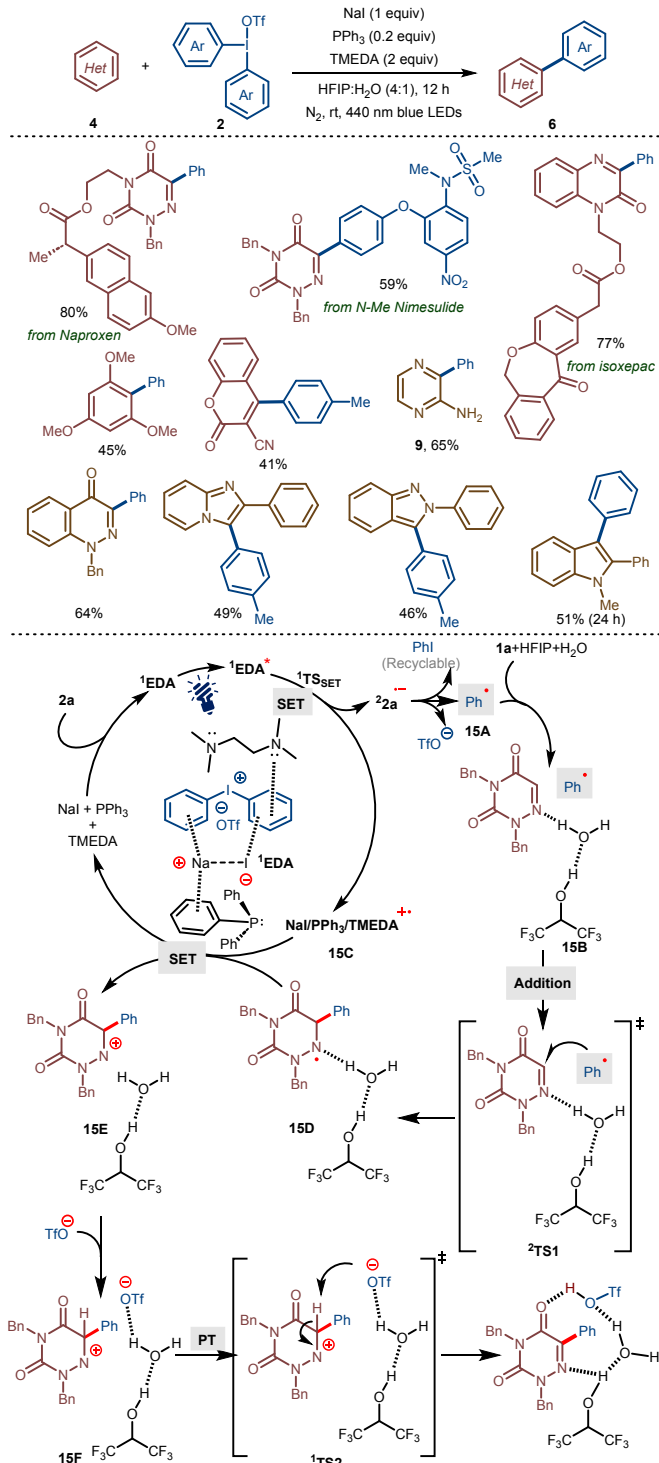
Scheme 14 Csp²–H arylation of pyrroles via charge-transfer complex formation

Traditional EDA complexes involving DAIRs were mostly restricted to electron-rich reacting partners serving as donors. Under these conditions, reacting partners (electron-rich donors and DAIRs) serve as a donor-acceptor pair, which results in the generation and recombination of resulting radicals due to the well-known cage effect.³² In 2023, the Murarka group developed an innovative strategy to generate aryl radicals from DAIRs by overcoming the cage effect through the formation of a unique multicomponent EDA complex (Scheme 15).^{6a} They discovered an inexpensive and efficient trimolecular donor system comprising NaI, PPh₃ and tetramethylethylenediamine (TMEDA), which forms a self-assembled tetrameric EDA complex with DAIRs. The resulting charge transfer complex furnishes aryl radicals upon irradiation with visible light. The strategy was successfully applied to the arylation of various electron-deficient and electron-rich heterocycles using a palette of densely functionalized DAIRs to furnish the respective arylated heterocycles in moderate to excellent yields. In general, twelve different classes of heterocycles, including azauracil, quinoxalinone, indole, cinnolinone, indazole, imidazopyridine, pyrazines, to name a few, were successfully arylated using the novel EDA technology. Additionally, the versatility of the method was showcased by its application to late-stage modifications of drug molecules, natural products, and pharmaceuticals. Based on detailed mechanistic investigations, comprising density functional theory (DFT) and time-dependent DFT (TD-DFT) calculations authors established the formation of a self-assembled ¹EDA complex between donor triad (NaI, PPh₃, TMEDA) and DAIRs featuring several non-covalent interactions (Scheme 15).

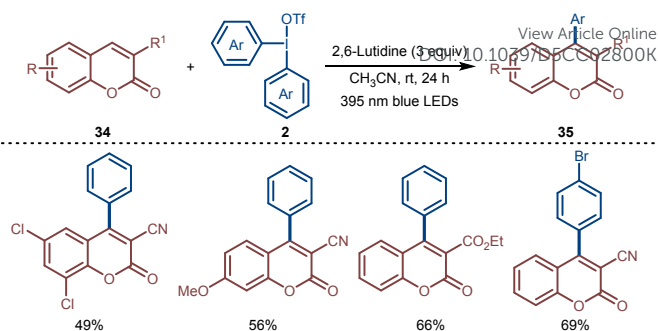
Upon irradiation, charge transfer between the nitrogen lone pair of TMEDA and the vacant π* orbital of the DPIT **2a** in the EDA leads to the generation of a phenyl radical **15A**. Notably, 1,1,1,3,3,3-Hexafluoro-2-propanol (HFIP) and H₂O play a crucial role in the stabilization of reactant complex **15B** and nucleophilic addition of the phenyl radical on azauracil through a long-chain hydrogen bonding network. The *N*-centred radical intermediate **15D** generated through the phenyl radical addition undergoes SET with the triad radical cation **15C**, regenerating the original donor triad system and a cationic intermediate **15E**. Finally, the triflate anion-assisted deprotonation delivers the desired phenylated azauracil.

Following a similar EDA-driven strategy, Reddy and co-workers subsequently reported a visible light-mediated selective C4-arylation of 2-oxo-2*H*-chromene-3-carbonitriles **34** with diaryliodonium reagents **2** using 2,6-lutidine as the donor molecule (Scheme 16).³³

The reaction proceeded through the formation of an EDA complex between DAIRs **2** and 2,6-lutidine, which, upon absorbing light, initiates a single-electron transfer (SET) process generating the aryl radical. Subsequent addition of the aryl radical to the C4 position of 2-oxo-2H-chromene-3-carbonitriles **34** provides the desired arylated products **35**.

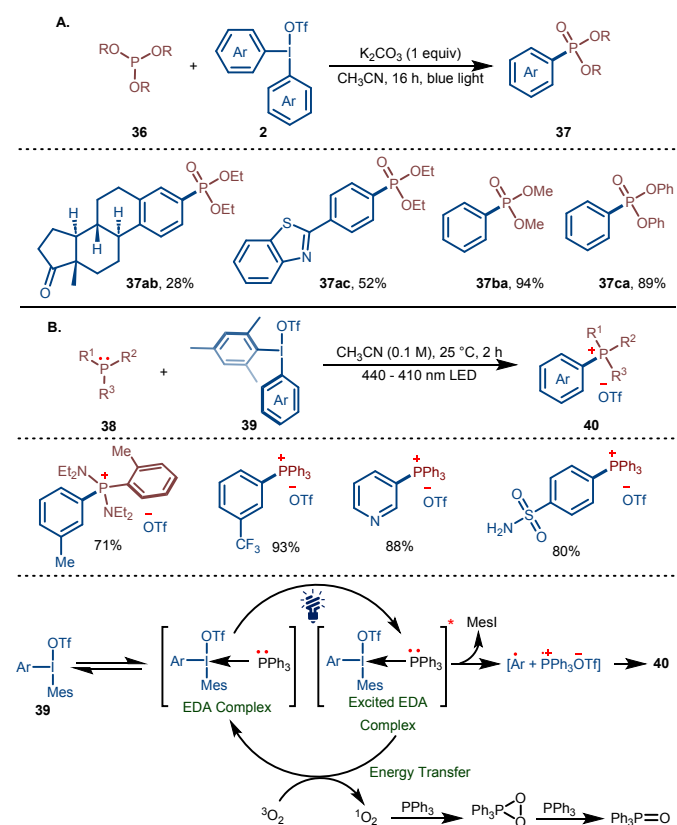


Scheme 15 Csp²-H Arylation of heterocycles through the formation of tetramolecular EDA complex



Scheme 16 Csp²-H arylation of 2-oxo-2H-chromene-3-carbonitriles via EDA complex formation

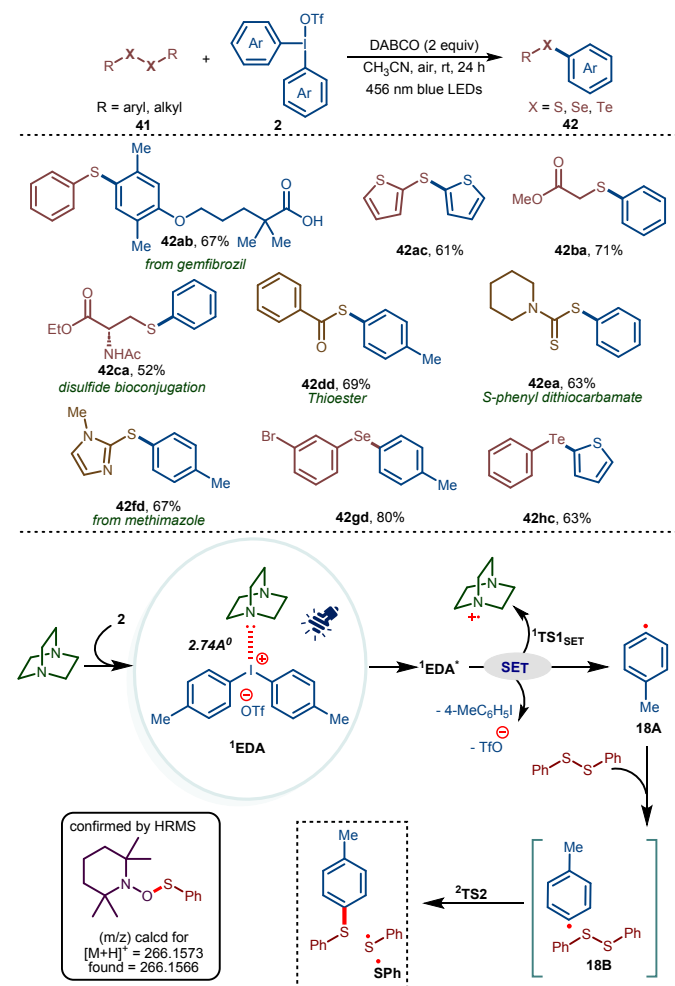
1.2.2 Csp²-X (X = P, S, Se, Te, B) Bond Formation



Scheme 17 Arylation of phosphite and tertiary phosphines via EDA complex formation

In 2018, Lakhdar and co-workers developed a straightforward synthesis to access aryl phosphonates **37** by reacting DAIRs **2** with phosphites **36** in the presence of potassium carbonate as a base under visible light irradiation (Scheme 17A).³⁴ The reaction demonstrated broad scope and was applicable to the synthesis of pharmaceutically relevant organophosphorus compounds. For example, steroid-derived phosphonate **37ab** and phosphonate-based calcium antagonist **37ac** were prepared in 28% and 52% yields, through reacting triethylphosphite with mesityl-derived corresponding non-symmetrical DAIRs. Based on detailed mechanistic studies and DFT calculations, the authors postulated that the reaction proceeds through the formation of a weak EDA complex between DAIRs **2** and phosphites **36**, where the complex is held together by a weak halogen bond. Later, Karchava and co-

workers developed a photoinduced method for the arylation of tertiary phosphines **38** using aryl(mesityl)iodonium triflates **39** to provide corresponding quaternary arylphosphonium salts **40** in moderate to good yields (Scheme 17B).³⁵ The transformation was enabled by a photoexcited EDA complex formation between tertiary phosphines **38** and DAIRs **39** under simple, robust, and metal-free conditions. The feasibility of introducing electronically diverse aryl groups, and compatibility of sterically congested tertiary phosphines are the salient features of this transformation. The proposed mechanism begins with forming a ground-state electron donor-acceptor (EDA) complex between triphenyl phosphine and DAIR **39**, which, upon irradiation with blue light, undergoes the SET process to generate an aryl radical and a phosphorus radical cation. Afterwards, a combination of these radical intermediates delivers the final phosphonium salts **40**. Additionally, an energy transfer process instead of a SET involving excited EDA in the presence of oxygen was suggested in the mechanism. In this pathway, the excited EDA complex transfers energy to triplet oxygen, producing singlet oxygen, which reacts with PPh₃ to yield Ph₃PO.



Scheme 18 Synthesis of (hetero)aryl chalcogenides via EDA complex formation

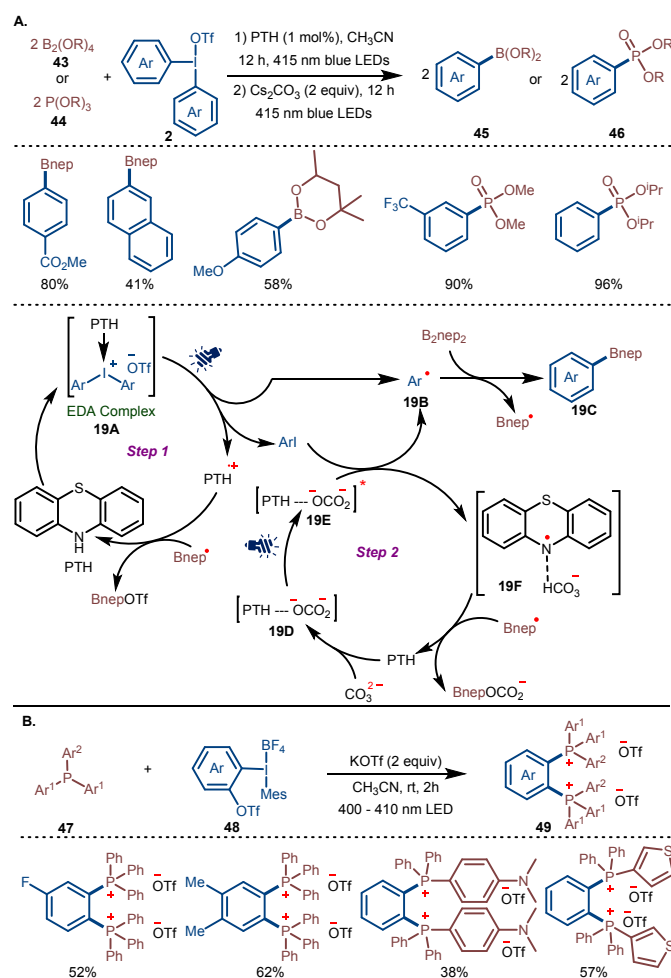
In 2024, Murarka and co-workers developed a visible-light-induced, scalable, and robust methodology to synthesize a variety of di(hetero)aryl and aryl/alkyl chalcogenides (C–S, C–Se, and C–Te) by reacting an array of DAIRs **2** and dichalcogenides **41** in the presence

of 1,4 diazabicyclo[2.2.2]octane (DABCO) as an inexpensive and readily available donor (Scheme 18).³⁶ The method featured a broad scope, appreciable functional group tolerance, and operated under open-to-air conditions. Notably, the method was applicable for late-stage functionalization of triglyceride-lowering drug, gemfibrozil (**42ab**, 67%), and enabled disulfide bioconjugations as demonstrated through preparation of bioconjugated thioether **42ca** (52%). Moreover, the chalcogenation technology facilitated access to biologically relevant thioesters **42dd**, dithiocarbamates **42ea**, and diverse pharmaceuticals under amenable conditions. Interestingly, the combined experimental and theoretical studies conducted with unsymmetrical DAIRs revealed that selective transfer of electron-rich and sterically congested aryl groups was preferred under photoinduced EDA conditions, due to the greater nucleophilicity of the resulting aryl radicals. Detailed mechanistic studies combined with DFT calculations provided insight into the reaction pathway. Initially, DABCO and DAIR associate to form a ground-state EDA complex **1EDA**. Upon irradiation, the EDA complex undergoes SET, generating the aryl radical **18A** with the release of aryl iodide. Then, the aryl radical **18A** interacts with the disulfide substrate to form an endergonic intermediate complex **18B**, which transitions through a transition state, forming the desired product and **SPh** radical. The formation of the **SPh** radical was confirmed by HRMS analysis.

Subsequently, Romero and co-workers introduced a photocatalyst-free approach for generating phenyl radical from DPIT using Lewis bases as activators.³⁷ They screened a variety of Lewis bases to optimize phenyl radical generation and successfully trapped it with B₂Pin₂, furnishing Ph-BPin. Based on UV-Vis studies, variable temperature (VT) ¹H NMR, kinetic experiments, and computational calculations, the authors established that simple Lewis bases can generate aryl radicals from DAIRs under visible light irradiation without the need for detectable halogen bonding interactions or coloured EDA complex formation.

In 2024, Wu and co-workers developed a one-pot photocatalytic method for the efficient arylation of boron- **43** and phosphorus-based **44** compounds using DAIRs **2** as aryl radical progenitors and phenothiazine (PTH) as the photocatalyst (Scheme 19A).³⁸ Based on mechanistic studies, it was proposed that the reaction begins with the formation of an electron donor-acceptor (EDA) complex **19A** between PTH and DAIR **2**, which, upon light excitation, undergoes a SET to generate an aryl radical **19B**, aryl iodide, and PTH^{•+}. The resulting aryl radical then reacts with B₂nep₂ to form final product **19C** and Bnep[•], which then reduces PTH^{•+} to PTH, thereby completing the first catalytic cycle. In the second cycle, Cs₂CO₃ is proposed to form a hydrogen-bonded complex **19D** with PTH, which, upon photoexcitation, undergoes proton-coupled electron transfer (PCET) with the previously generated aryl iodide to generate aryl radical **19B**, and an oxidized PTH species **19F**. Thus, generated aryl radical again reacts with B₂nep₂ to generate final product **19C**, and this catalytic cycle gets completed in a similar manner to the first catalytic cycle. Overall, this is an interesting report where both the aryl groups of DAIRs were effectively translated to the corresponding products. Recently, the Han group reported a visible light-driven vicinal difunctionalization of ortho-trifluoromethanesulfonylated DAIRs **48** using readily available tertiary phosphines to furnish sterically hindered bis-(tetraarylphosphonium) salts **49** in moderate to good yields (Scheme 19B).³⁹ The reaction was proposed to

proceed through the formation of an EDA complex between DAIRs **48** and triarylphosphines **47**.



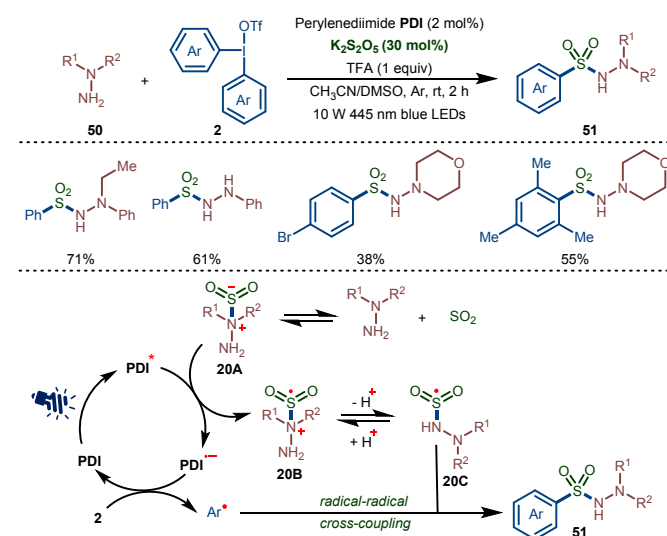
Scheme 19 Borylation, Phosphorylation and vicinal difunctionalization of diaryliodonium reagents via EDA complex formation

2. Multicomponent Reactions

2.1 Csp²-S Bond Formation

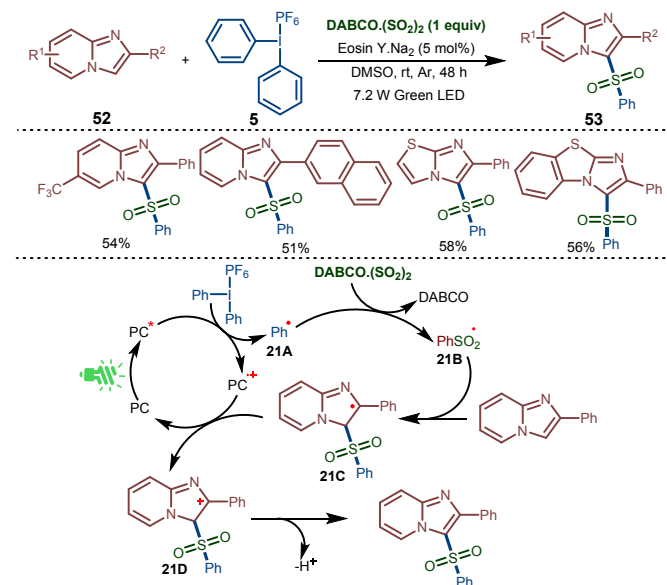
In 2017, Manolikakes and co-workers developed a visible light photoredox-catalyzed aminosulfonylation of DAIRs **2** under mild conditions (Scheme 20).⁴⁰ This multi-component approach enabled the synthesis of *N*-aminosulfonamides **51** using commercially available perylenediimide as the photocatalyst along with hydrazines **50**, sulfur dioxide (SO₂), and DAIRs **2** as the reacting partners. In this method, SO₂ was introduced either as a solid amine complex DABCO·(SO₂)₂ or generated *in situ* via acid-mediated decomposition of bisulfite. According to the proposed mechanism, initially, hydrazines and sulfur dioxide form a stable hydrazine-sulfur dioxide adduct **20A**. Subsequently, reductive quenching of the excited photocatalyst PDI* with the adduct **20A** furnishes radical cation **20B** and the reduced catalyst. The reduced photocatalyst is reductive enough to generate aryl radical from DAIRs **2** while regenerating the ground state photocatalyst. Meanwhile, deprotonation of intermediate **20B** affords sulfonyl radical **20C**, which upon radical-radical coupling with aryl radicals furnishes the final product **51**.

Subsequently, a similar photocatalytic multicomponent strategy was adopted for synthesizing thiosulfonates in moderate to good yields through a reaction of thiols, DABSO, and DAIRs.⁴¹ The reaction proceeds through radical-radical cross-coupling of sulfenyl radicals and *in situ* generated arylsulfonyl radicals.



Scheme 20 Visible light-driven multicomponent reaction for aminosulfonylation of DAIRs

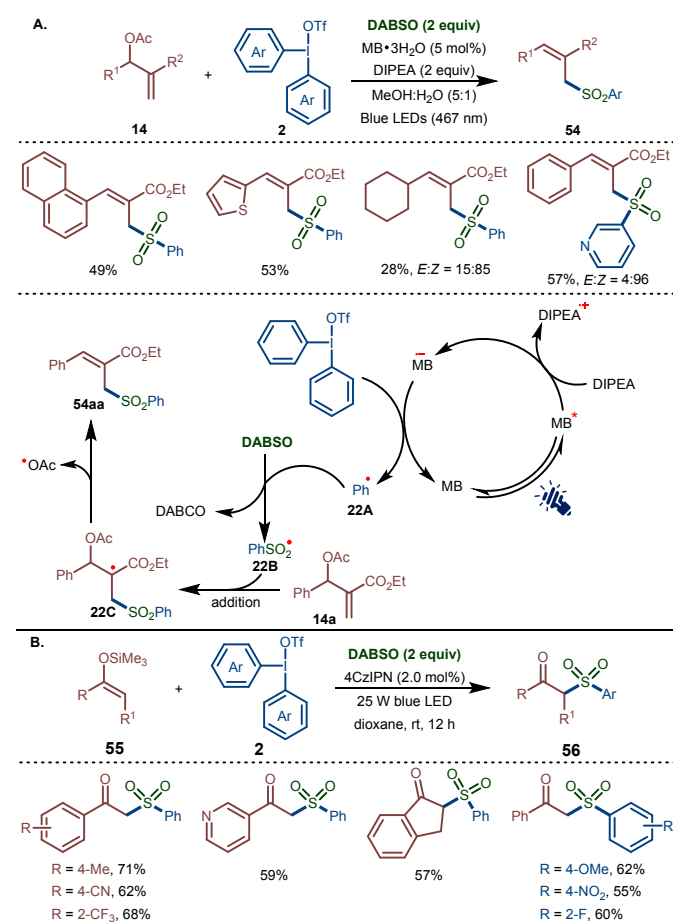
In 2020, Piguel and co-workers developed a photocatalytic multicomponent method for the aryl sulfonylation of imidazoheterocycles **52** through an overall C-H functionalization process (Scheme 21).⁴² This method utilized Eosin Y.Na₂ as the photocatalyst, diaryliodonium reagents **5** as the aryl precursor, and DABCO·(SO₂)₂ as the SO₂ source to provide C-3 sulfonylated imidazoheterocycles **53** in moderate to good yields. The phenyl radical **21A** generated through oxidative quenching of the excited photocatalyst with diphenyliodonium salt gets captured by DABSO to form phenylsulfonyl radical **21B**, which, upon regioselective addition to the imidazoheterocycle, delivers the final product.



Scheme 21 Visible light-driven aryl sulfonylation of imidazoheterocycles

The Murarka group successfully extended their study on the organophotoredox-catalyzed arylation of MBH acetates **14** to the aryl sulfonation of MBH acetates using DABSO as the SO₂ surrogate (Scheme 22A).²¹ The phenyl radical **22A** generated under the reaction conditions was captured by DABSO, leading to the formation of a phenyl sulfonyl radical **22B**, which then reacted with MBH acetate **14a** to yield the final phenylsulfonylated product **54aa**. The reaction demonstrated a broad scope, where a diverse variety of DAIRs **2**, (hetero)aromatic and aliphatic aldehyde-derived MBH acetates **14** and DABSO underwent multicomponent reaction to provide the desired allylic aryl sulfones **54** with high Z-stereoselectivity.

Later, a versatile multicomponent approach involving DAIRs **2**, DABSO, and silyl enolates **55**, enabling the synthesis of various β -keto sulfones **56** under mild conditions, was documented (Scheme 22B).⁴³ This strategy showcased noteworthy substrate diversity and high tolerance for various functional groups. Notably, the use of β -alkyl-substituted silyl enolates in the reaction enabled the formation of α -alkyl-substituted β -keto sulfones, which could not be achieved through prior SO₂ insertion methods.

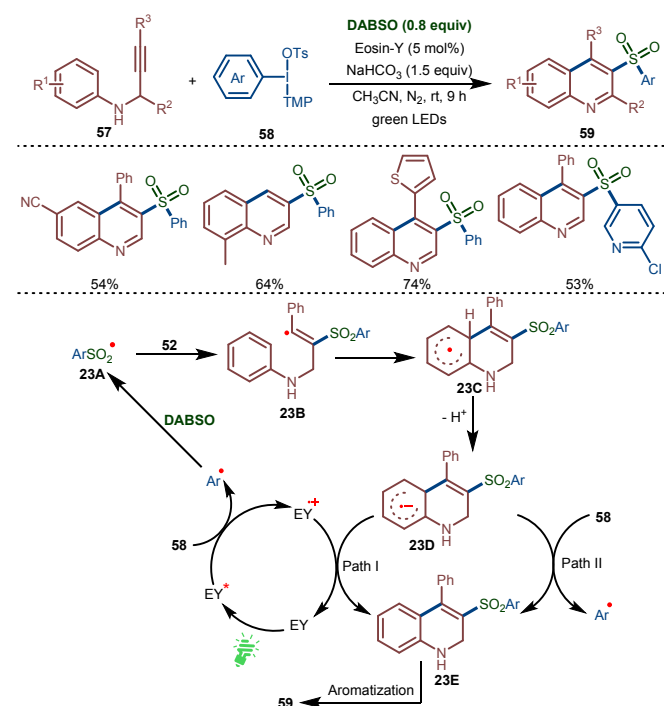


Scheme 22 Visible light-mediated arylsulfonation of MBH acetates and silyl enolates

2.2 Cascade Annulation

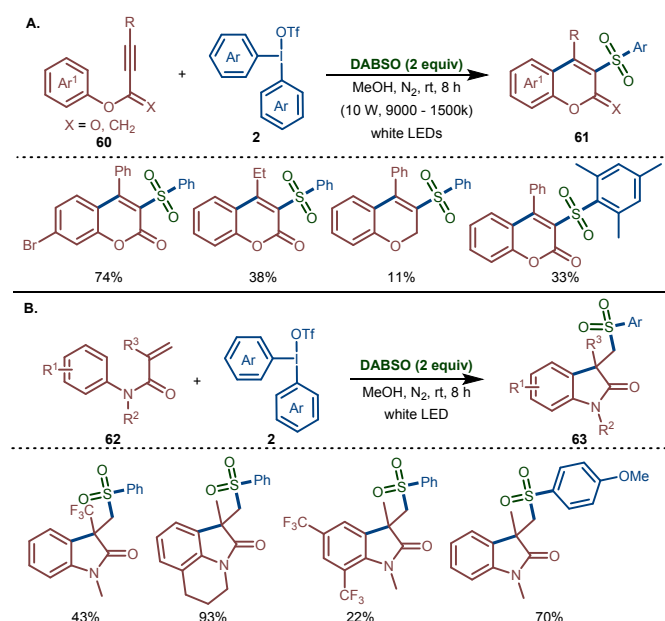
In 2018, Zhang and co-workers developed an Eosin Y photoredox-catalyzed three-component approach involving *N*-propargyl aromatic amines **57**, DAIRs **58**, and DABSO for synthesizing 3-

arylsulfonylquinolines **59** (Scheme 23).⁴⁴ The reaction provides an efficient way to construct the quinoline core while concurrently forging C-S and C-C bonds. The reaction was scalable and demonstrated broad scope and high functional group tolerance. Mechanistically, the process begins with the excited photocatalyst reducing DAIRs **58** to generate **EY⁺**, and aryl radicals that are captured by DABSO, forming corresponding arylsulfonyl radicals **23A**. Afterwards, the sulfonyl radicals undergo intermolecular regioselective addition to the *N*-propargyl aromatic amines **57** to produce alkenyl radical intermediate **23B**. **23B** then undergoes intramolecular cyclization to generate radical intermediate **23C**, which upon deprotonation produces radical anion **23D**. The intermediate **23D** is oxidized by **EY⁺** or DAIR **58** to form 1,2-dihydroquinoline **23E**. Finally, dehydroaromatization of intermediate **23E** produces the desired 3-arylsulfonylquinoline product **59**.



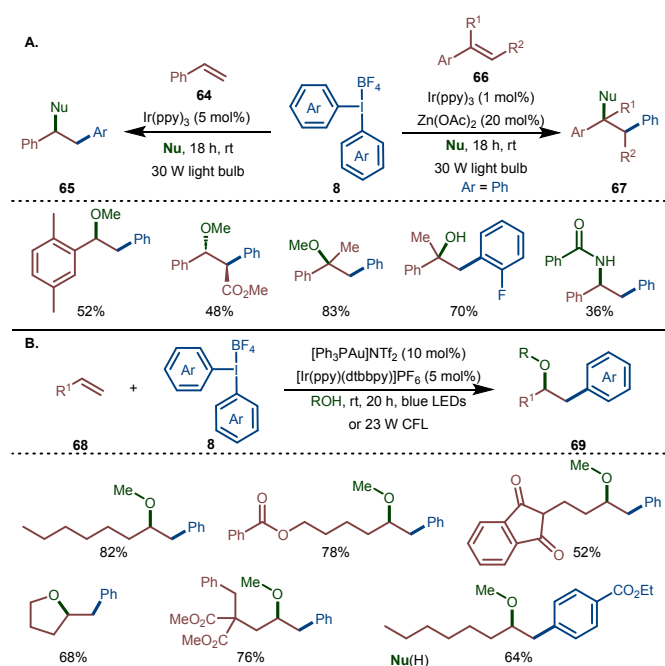
Scheme 23 Synthesis of sulfonylated quinolines through cascade annulation strategy

Manolikakes and co-workers successfully developed a visible light-induced photocatalyst-free three-component approach to access sulfonylated coumarins⁴⁵ and oxindoles.⁴⁶ While in both reactions, DAIRs **2** served as aryl radical surrogates, and DABSO as the sulfur dioxide precursor, the synthesis of sulfonylated coumarins **61** and oxindole derivatives **63** employed phenylpropynoates **60**, and *N*-arylacrylamides **62** as starting materials in a respective manner (Scheme 24A and 24B). These reactions proceed through the formation of a charge-transfer complex between DABSO and DAIR **2**, which facilitates the generation of aryl radicals. In general, both reactions proceeded under amenable conditions, furnishing corresponding products in moderate to good yields. Subsequently, a photoinduced sulfonylative spirocyclization involving *N*-arylacrylamides, DAIRs, and DABSO, enabling access to azaspiro[4.5]-trienones, was reported as well.⁴⁷



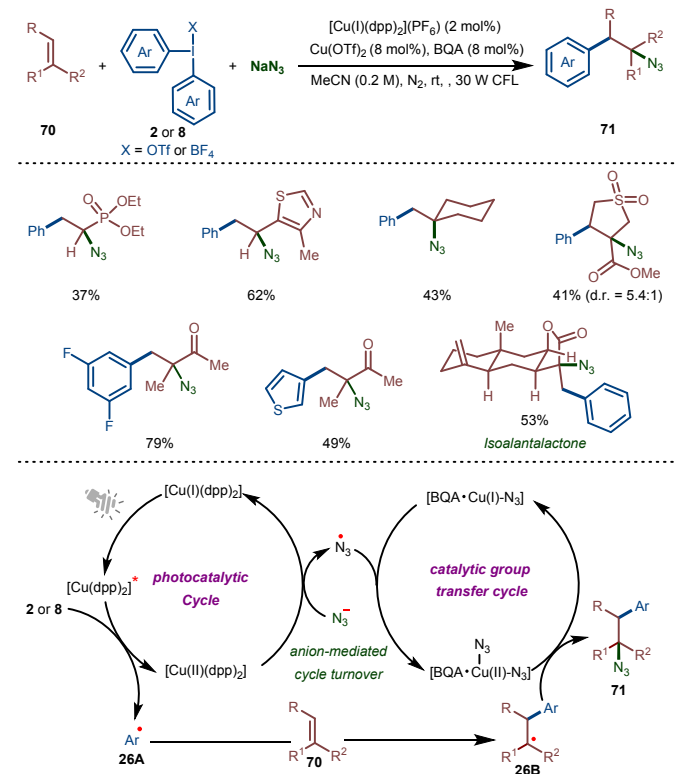
Scheme 24 Photoinduced Cascade cyclization for the synthesis of sulfonfylated coumarins and oxindoles

2.3 Difunctionalization of Alkenes



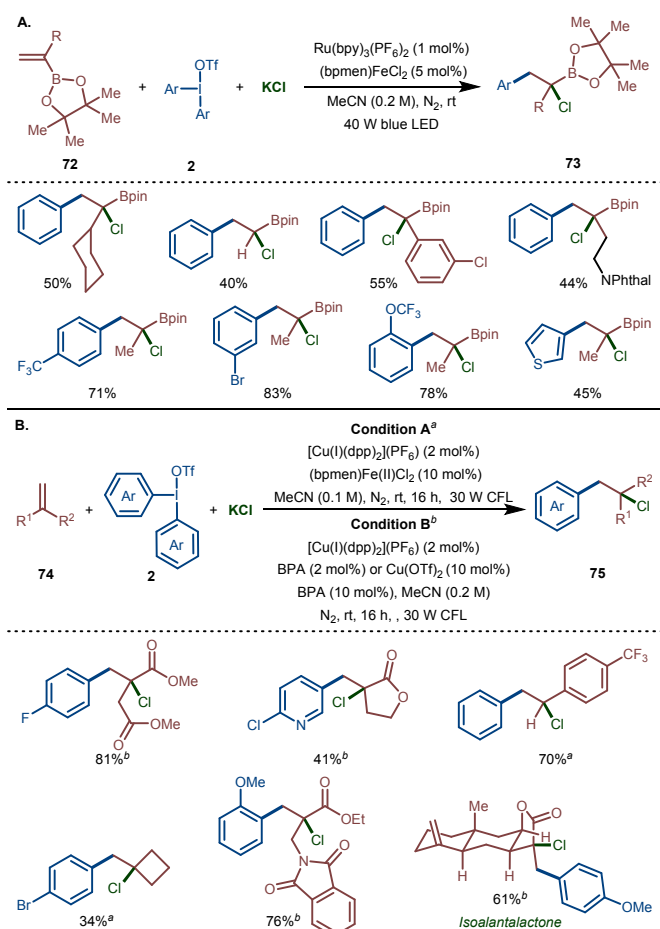
Scheme 25 Visible light-driven difunctionalization of styrenes and alkenes
DOI: 10.1039/D5CC02800K

In 2013, Greaney and co-workers developed an innovative photoredox-catalyzed three-component coupling between styrenes **64** or **66**, DAIRs **8**, and nucleophiles such as alcohols, nitriles, or water to accomplish difunctionalization across the styrene double bond (Scheme 25A).⁴⁸ The reaction proceeds through a simple radical-polar cross-over mechanism, where the benzylic radical generated through the addition of an aryl radical on styrene gets oxidized to the cation, which, after trapping with the appropriate nucleophile, affords the desired coupled products **65** or **67**. Later, the Glorius group developed a dual gold and iridium photocatalytic system to achieve intermolecular three-component oxyarylations of simple alkenes **68** using diaryliodonium compounds **8** as the arene coupling partner (Scheme 25B).⁴⁹ In general, a variety of non-activated terminal alkenes reacted with several diaryliodonium salts and alcohols to provide respective homobenzy-substituted ethers **69** in moderate to good yields. The reaction begins with the activation of the alkene by coordination to the gold catalyst, followed by the nucleophilic attack by aliphatic alcohol, leading to the formation of alkyl gold intermediate **25A**. Meanwhile, the aryl radical is generated via oxidative quenching of the excited Ir-photocatalyst, accompanied by the formation of aryl iodide as a by-product. The aryl radical subsequently reacts with the gold(I) intermediate **25A**, oxidizing it to a gold(II) species **25B**. Afterwards, **25B** gets further oxidized to gold(III) species **25C** by the oxidized photocatalyst and completes the photocatalytic cycle. Finally, reductive elimination from the gold(III) species **25C** produces the desired oxyarylated products **69** and regenerates the gold(I) catalyst.



Scheme 26 Dual catalytic azidoarylation of alkenes

In 2021, the Gaunt group developed a conceptually innovative dual-catalytic platform for the difunctionalization of alkenes **70** using diaryliodonium salts **2** or **8** as aryl radical precursors under visible light irradiation.⁵⁰ In this process, the incipient homobenzylic radical **26B** formed upon addition of the aryl radical **26A** was captured by an anionic nucleophile through a separate transition metal-catalyzed group transfer catalytic cycle. Authors utilized a highly effective dual catalysis system comprising [Cu(dpp)₂](PF₆) as a photocatalyst (dpp=2,9-diphenyl-1,10-phenanthroline) and BQA•Cu(OTf)₂ (BQA=N-*tert*-butyl-1-(quinolin-2-yl)methanimine) to execute azido-arylation of a variety of alkenes using sodium azide as the azide source (Scheme 26).⁵⁰ The multicomponent modular approach provided access to functionally diverse β-arylethylamines in moderate to good yields. Mechanistically, the reaction begins with aryl-radical **26A** generation through oxidative quenching of the excited Cu(I) photocatalyst with DAIR **2** or **8**, which upon addition to the alkene **70** forms homobenzylic radical intermediate **26B** (Scheme 25). Meanwhile, the second copper catalyst sequesters the azide anion by ligand substitution leading to the generation of two discrete catalytic cycles [Cu(II)(dpp)₂]²⁺ (from photocatalyst A) and a putative [BQA•Cu(I)-N₃] complex (from catalyst B), which require reduction and oxidation, respectively, to regenerate the active catalysts. The reduction of Cu(II)-photocatalyst by sodium azide regenerates Cu(I) photocatalyst, and the resulting azide radical adds to [BQA•Cu(I)-N₃], to form BQA•Cu(II)(N₃)₂. Finally, the azido group transfers from this Cu(II)-N₃ complex to the intermediate **26B**, delivering the desired products **71**.



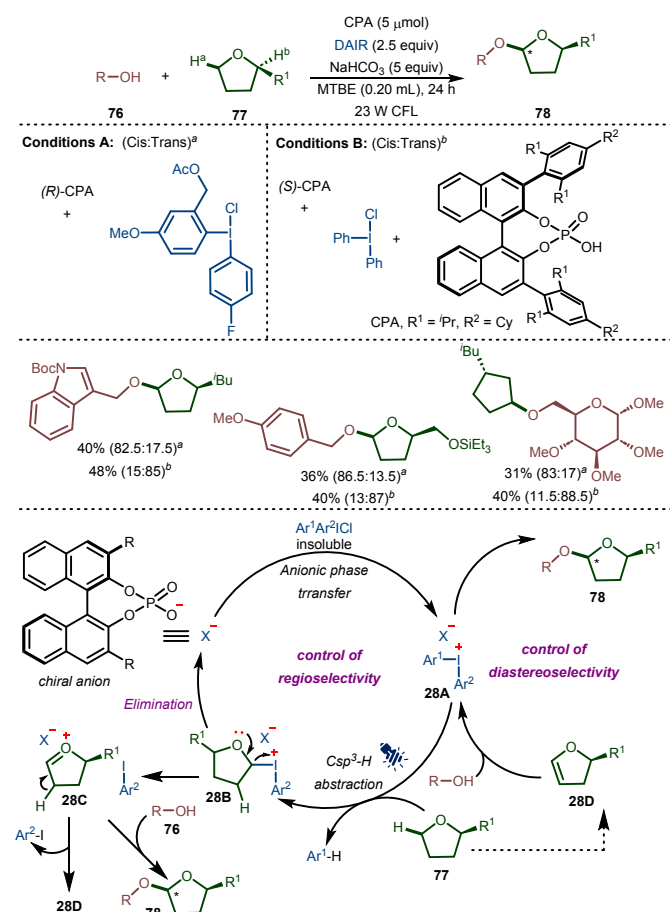
Scheme 27 Aryl-chlorination of vinyl boronic esters and alkenes via dual photoredox catalysis
DOI: 10.1039/D5CC02800K

Subsequently, the research group utilized a conceptually similar dual catalytic platform to develop the aryl-chlorination of vinyl boronic esters **72** using [Ru(bpy)₃](PF₆)₂ (bpy=2,2'-bipyridine) as photocatalyst and [(bpmen)FeCl₂] (bpmen=N,N-dimethyl-N,N-bis(pyridin-2-ylmethyl) ethane-1,2-diamine) as the atom-transfer precatalyst, leading to the synthesis of diverse α-chloro alkylboronic esters **73** (Scheme 27A).⁵¹ The reaction demonstrated a broad reaction scope, and the final products were amenable to a broad variety of synthetic diversification. The author's subsequent attempt to expand the scope beyond vinyl boronic esters led to the development of two distinct dual catalytic systems enabling efficient aryl-chlorination of electronically and structurally diverse alkenes **74** bearing a broad range of functional groups (Scheme 27B).⁵² While a copper-based photocatalyst was employed across all kinds of alkenes, different group-transfer catalysts were utilized depending on the substrate type. An iron(II) catalyst was utilized for styrenes and non-activated alkenes, and a pyridylimine-ligated copper complex served as the chlorine-transfer catalyst for electron-deficient alkenes. In general, the reaction demonstrated a broad substrate scope and exceptional tolerance to diverse functional groups.

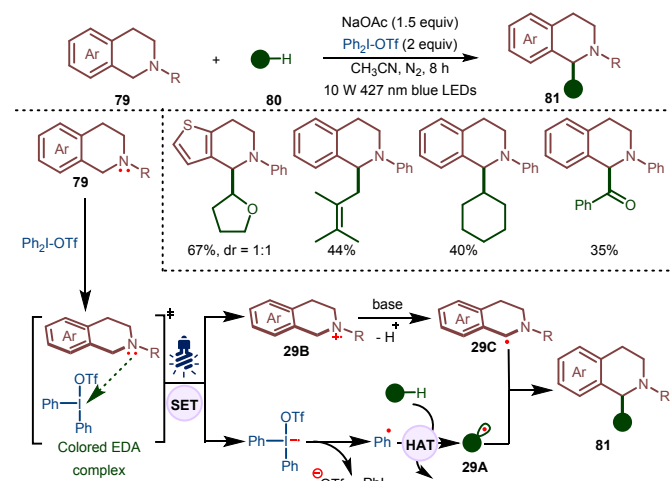
3. Hydrogen Atom Transfer (HAT)

The hydrogen atom transfer (HAT) process specifically depends upon the transfer of one proton and one electron simultaneously from one group to another group.^{10, 53} This process enables direct functionalization of R-H (R = C, Si, etc.) bonds in organic molecules in one single step for synthesizing many complex molecules. Traditionally, HAT methods require a stoichiometric amount of reagents and harsh reaction conditions, which limits the functioning of the HAT process. Recently, the visible light-mediated HAT method has evolved as an efficient platform for functionalizing direct R-H bonds by overcoming the limitation of redox potentials. In this section, we have discussed photoinduced HAT processes mediated by aryl radicals utilizing diaryliodonium reagents as HAT reagents.

In 2018, the Toste group documented a unique approach for the stereoselective α-C(sp³)-H acetalization of cyclic ethers **77** by integrating the photochemical feature of DAIRs with anionic phase-transfer catalysis (Scheme 28).⁵⁴ The chiral phosphate catalyst played a key role in controlling diastereoselectivity, enabling access to both *trans*- and *cis*-acetals **78** under mild conditions. Based on various mechanistic experiments, a plausible mechanism of this reaction was proposed. The reaction begins with an anionic phase transfer process, converting diaryliodonium chloride into chiral diaryliodonium phosphate **28A** in the presence of chiral phosphate anion. This intermediate facilitates hydrogen atom abstraction from tetrahydrofuran under visible-light irradiation, generating **28B**, which further disintegrates to iodoarene, chiral phosphate anion, and oxonium intermediate **28C**. Finally, the reaction of oxonium intermediate **28C** with alcohol **76** delivers the final product **78** with defined stereoselectivity.



Scheme 28 Light-driven α -C(sp³)-H acetalization of cyclic ethers using chiral diaryliodonium phosphates

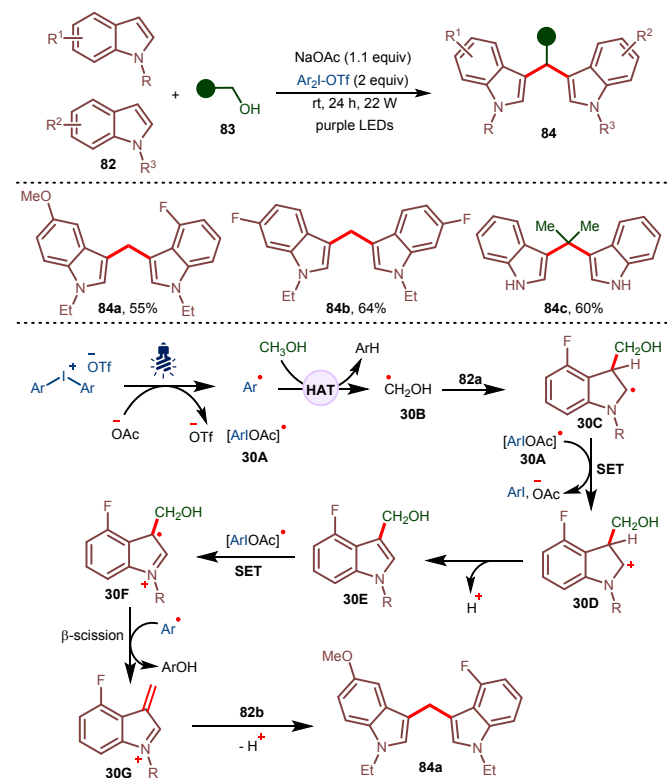


Scheme 29 C(sp³)-C(sp³) radical-radical cross-coupling via intermolecular HAT

Shi and co-workers presented a photocatalyst-free cross-dehydrogenative C(sp³)-C(sp³) and C(sp³)-C(sp²) radical-radical cross-coupling facilitated by an intermolecular hydrogen atom transfer (HAT) process (Scheme 29).⁵⁵ The strategy enabled efficient cross-coupling of α -N C(sp³)-H of amines with C(sp³)-H of both activated and non-activated aliphatic substrates **80**, including ethers, allylic and benzylic systems, simple cycloalkanes, and C(sp²)-H of

aldehydes, and amide to provide the corresponding products **81** in moderate to good yields. Following the formation of a phenyl radical through EDA complex formation, it undergoes HAT with **80** to generate corresponding C-centered radicals **29A**. Finally, radical radical cross-coupling between **29A** and benzylic radicals **29C** derived from tetrahydroisoquinoline provides the desired cross-coupled product **81**. Notably, in the absence of C-H partners, a direct coupling of the phenyl radical and α -N C(sp³)-H of amines was observed.

Huang and co-workers reported a novel strategy for the synthesis of both unsymmetrical and symmetrical bis(indolyl)methanes **84**, where a diaryliodonium reagent enabled the coupling of simple indoles **82** with alcohols **83** under visible-light irradiation (Scheme 30).⁵⁶ In this process, DAIR enabled photoinduced HAT from alcohols for the formation of corresponding hydroxy alkyl radicals. Mechanistically, the reaction begins with the disintegration of DAIR under visible light irradiation to generate an aryl radical, which then abstracts a hydrogen atom from methanol via HAT to furnish hydroxymethyl radical **30B**. Afterwards, regioselective addition of nucleophilic hydroxymethyl radical to electron-deficient indole **82a** provides intermediate **30C**, which upon single-electron oxidation by the radical intermediate **30A** forms a cationic species **30D**. Subsequent, β -Hydride elimination from **30D** affords indole-3-carbinol **30E**, which after successive SET oxidation and β -scission produces intermediate **30G**. Finally, interception of **30G** by electron-rich indole **82b** furnishes the desired product **84a**.

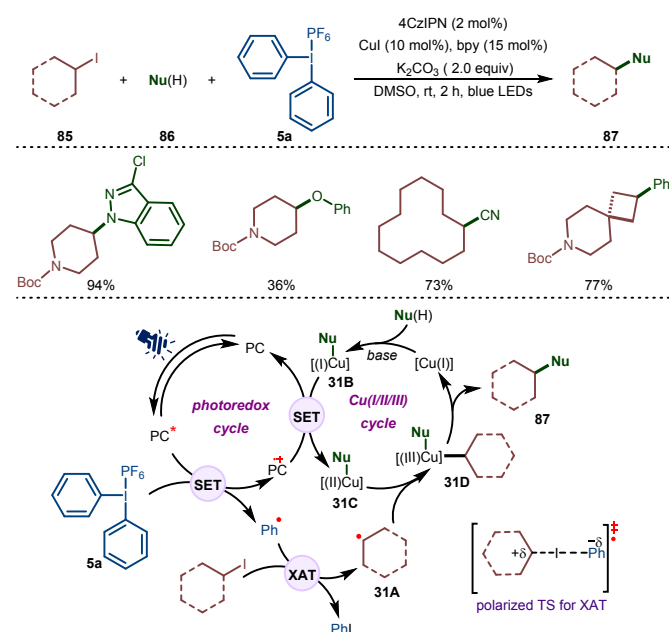


Scheme 30 Synthesis of bis(indolyl)methanes via diaryliodonium reagent-mediated HAT

4. Halogen Atom Transfer (XAT)

Halogen atom transfer (XAT) primarily relies on the bond dissociation energy (BDE) and the polarizability of the carbon-halogen (C–X) bond.¹¹ In this process, a specific abstractor radical extracts the halogen atom from the C–X bond via homolytic cleavage. Recently, XAT has garnered significant attention as it is independent of the redox potentials of alkyl halides.⁵⁷ The subsequent discussion focuses on aryl radical-mediated C–X bond activation strategies utilizing DAIRs as XAT reagents.

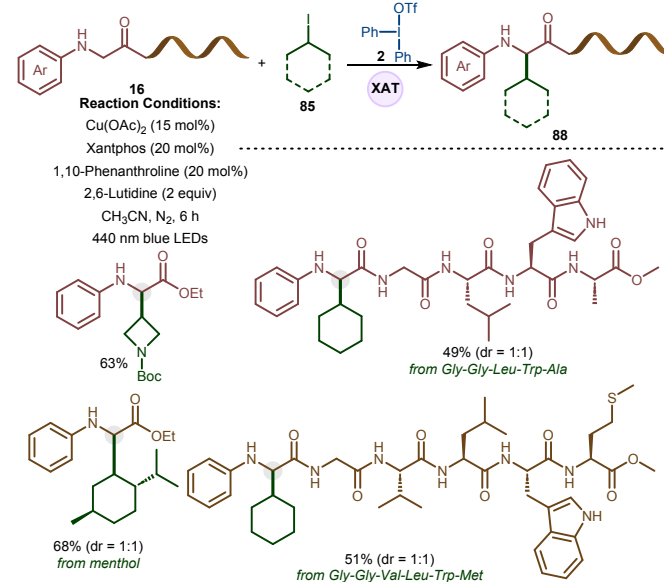
In 2023, Leonori and co-workers developed a novel toolbox strategy for the functionalization of alkyl iodides **85** with N-, O-, and C-based nucleophiles **86** using aryl radical-mediated halogen-atom transfer (XAT) process under visible light irradiation (Scheme 31).⁵⁸ The method utilized organic dye 4CzIPN and CuI as the catalytic dyad, and diaryliodonium reagent **5a** as the halogen abstractor for the XAT process. The merging of aryl radical-mediated XAT with copper catalysis provided a modular and divergent approach to assemble C(sp³)–N/O/C bonds under mild conditions. The proposed mechanism begins with the excited photocatalyst generating a phenyl radical from DAIR **5a**, leaving iodoarene as a by-product. The phenyl radical then undergoes a rapid XAT process with alkyl iodide **85**, producing the corresponding alkyl radical **31A**. Simultaneously, the base-assisted *in situ* generated Cu(I)–Nu species **31B** undergoes SET with the oxidized photocatalyst completing the photoredox cycle and forming intermediate **31C**. Finally, intermediates **31A** and **31C** combine to form intermediate **31D** which upon reductive elimination delivers the desired product **87**.



Scheme 31 Merger of XAT and Cu-catalysis for the cross-coupling of alkyl iodides with nucleophiles

In 2024, the Murarka group successfully demonstrated that copper-photoredox-catalyzed SET strategy can be merged with the XAT process in the presence of alkyl iodides to accomplish site-selective α -Csp³–H alkylation of glycines and peptides. In this synergistic SET/XAT approach, phenyl radicals generated from diphenyl iodonium triflate were subsequently employed in an XAT process to produce alkyl radicals from alkyl iodides **85** (Scheme 32).²⁴ The method exhibited broad scope and excellent functional group

tolerance, facilitating access to a variety of α -alkylated glycines and peptides under ambient conditions. The mechanism is along the lines of the arylation of glycines and peptides described in Scheme 8. Subsequent to its generation, the phenyl radical reacts with alkyl iodides to generate alkyl radicals through an XAT process, which upon radical-radical coupling with α -amino carbon radicals, results in the desired alkylated product **88**.



Scheme 32 Site-selective Csp³–H alkylation of glycines and peptides via copper-photoredox catalysis

Conclusion and Outlooks

In this feature article, we have summarized the significant advancements, including contributions from our research group, in visible light-mediated transformations using diaryliodonium reagents as aryl radical surrogates. Due to the affordability, ease of handling, and stability at room temperature, this class of reagents has garnered applications in a variety of synthetic transformations, such as C(sp²)–H and C(sp³)–H arylations, allylic arylations, and cascade annulations. Besides two-component reactions, they also participate in various multicomponent reactions, including alkene difunctionalizations under photoinduced conditions, providing access to biologically relevant and structurally important building blocks in an efficient manner. Although the full industrial potential of diaryliodonium reagents under photoinduced conditions has yet to be fully realized, the examples presented in this feature article underscore their growing significance in academic research. Continued development of milder and more sustainable photocatalytic methodologies is expected to further enhance the applicability of these reagents, potentially extending their relevance to industrial settings upon appropriate optimization. Despite this tremendous development and growing interest in this area, there are many opportunities for future research. For example, novel strategies should be devised to utilize the released iodoarene in an effective manner through innovative radical-

polar cross-over reactions. The foreseeable future should witness the development of a variety of asymmetric cross-couplings involving DAIRs. Moreover, the development of novel synthetic strategies to prepare di(hetero)aryliodonium salts from complex natural products, heterocycles, and bioactive compounds will certainly boost the popularity of this class of compounds. Nevertheless, we hope this feature article will further stimulate the interest of the audience towards the discovery of new reaction paradigms involving DAIRs under visible light irradiation.

Data availability

No primary research results, software or code have been included, and no new data were generated or analysed as part of this review.

Author Contributions

The manuscript was written through the contributions of all authors. All authors have given approval to the final version of the manuscript.

Conflicts of interest

There are no conflicts to declare.

Acknowledgements

SM acknowledges ANRF [CRG/2022/000470] for funding and DST-FIST [SR/FST/CS-II/2019/119(C)] for the HRMS facility at IIT Jodhpur.

Notes and references

- (a) K. Aradi, B. L. Tóth, G. L. Tolnai and Z. Novák, *Synlett*, 2016, **27**, 1456-1485; (b) E. A. Merritt and B. Olofsson, *Angew. Chem., Int. Ed.*, 2009, **48**, 9052-9070.
- (a) A. Yoshimura and V. V. Zhdankin, *Chem. Rev.*, 2024, **124**, 11108-11186; (b) S. K. Parida, S. Jaiswal, P. Singh and S. Murarka, *Org. Lett.*, 2021, **23**, 6401-6406; (c) J. Malmgren, S. Santoro, N. Jalalian, F. Himo and B. Olofsson, *Chem. – Eur. J.*, 2013, **19**, 10334-10342; (d) Z. Gonda and Z. Novák, *Chem. – Eur. J.*, 2015, **21**, 16801-16806; (e) R. Ghosh, E. Lindstedt, N. Jalalian and B. Olofsson, *ChemistryOpen*, 2014, **3**, 54-57; (f) T. Dohi, M. Ito, N. Yamaoka, K. Morimoto, H. Fujioka and Y. Kita, *Angew. Chem., Int. Ed.*, 2010, **49**, 3334-3337; (g) D. I. Bugaenko, M. A. Yurovskaya and A. V. Karchava, *Org. Lett.*, 2018, **20**, 6389-6393; (h) D. I. Bugaenko, A. A. Volkov, V. V. Andreychev and A. V. Karchava, *Org. Lett.*, 2023, **25**, 272-276; (i) M. Bielawski, M. Zhu and B. Olofsson, *Adv. Synth. Catal.*, 2007, **349**, 2610-2618; (j) S. Jaiswal, S. K. Parida, S. Murarka and P. Singh, *Bioorg. Med. Chem.*, 2022, **68**, 116874.
- T. Dohi, M. Ito, N. Yamaoka, K. Morimoto, H. Fujioka and Y. Kita, *Tetrahedron*, 2009, **65**, 10797-10815.
- (a) H. Zhao, V. D. Cuomo, W. Tian, C. Romano and D. J. Procter, *Nature Reviews Chemistry*, 2025, **9**, 61-80; (b) X.-Q. Xie, W. Zhou, R. Yang, X.-R. Song, M.-J. Luo and Q. Xiao, *Org. Chem. Front.*, 2024, **11**, 4318-4342; (c) N. Kvasovs and V. Gevorgyan, *Chem. Soc. Rev.*, 2021, **50**, 2244-2259; (d) I. Ghosh, L. Marzo, A. Das, R. Shaikh and B. König, *Acc. Chem. Res.*, 2016, **49**, 1566-1577.
- (a) I. K. Sideri, E. Voutyritsa and C. G. Kokotos, *Org. Biomol. Chem.*, 2018, **16**, 4596-4614; (b) M. H. Shaw, J. Twilton and D. W. C. MacMillan, *J. Org. Chem.*, 2016, **81**, 6898-6926; (c) N. A. Romero and D. A. Nicewicz, *Chem. Rev.*, 2016, **116**, 10075-10166; (d) C. K. Prier, D. A. Rankic and D. W. C. MacMillan, *Chem. Rev.*, 2013, **113**, 5322-5363; (e) J. M. R. Narayanam and C. R. J. Stephenson, *Chem. Soc. Rev.*, 2011, **40**, 102-113; (f) S. Kumar Hota, D. Jinan, S. Prakash Panda, R. Pan, B. Sahoo and S. Murarka, *Asian J. Org. Chem.*, 2021, **10**, 1848-1860; (g) C. Pan, D. Chen, Y. Cheng and J.-T. Yu, *Chem. Commun.*, 2024, **60**, 4451-4454; (h) X. Zou, Y. Lang, X. Han, M.-W. Zheng, J. Wang, C.-J. Li and H. Zeng, *Chem. Commun.*, 2024, **60**, 2926-2929; (i) Y. Sun, L. Yang, Y. Cheng, G. An and G. Li, *Chin. Chem. Lett.*, 2024, **35**, 109250; (j) L. Yang, H. Xie, G. An and G. Li, *J. Org. Chem.*, 2021, **86**, 7872-7880.
- (a) P. Meher, S. P. Panda, S. K. Mahapatra, K. R. Thombare, L. Roy and S. Murarka, *Org. Lett.*, 2023, **25**, 8290-8295; (b) P. P. Romańczyk and S. S. Kurek, *Electrochimica Acta*, 2020, **351**, 136404.
- F. Herbrink, P. Camarero González, M. Krstic, A. Puglisi, M. Benaglia, M. A. Sanz and S. Rossi, *Applied Sciences*, 2020, **10**, 5596.
- (a) L. van Dalsen, R. E. Brown, J. A. Rossi-Ashton and D. J. Procter, *Angew. Chem., Int. Ed.*, 2023, **62**, e202303104; (b) A. K. Wortman and C. R. J. Stephenson, *Chem*, 2023, **9**, 2390-2415; (c) Y. Sumida and H. Ohmiya, *Chem. Soc. Rev.*, 2021, **50**, 6320-6332; (d) C. G. S. Lima, T. de M. Lima, M. Duarte, I. D. Jurberg and M. W. Paixão, *ACS Catal.*, 2016, **6**, 1389-1407; (e) G. E. M. Crisenza, D. Mazzarella and P. Melchiorre, *J. Am. Chem. Soc.*, 2020, **142**, 5461-5476.
- D. R. Stuart, *Chem. – Eur. J.*, 2017, **23**, 15852-15863.
- H. Cao, X. Tang, H. Tang, Y. Yuan and J. Wu, *Chem Catalysis*, 2021, **1**, 523-598.
- F. Juliá, T. Constantin and D. Leonori, *Chem. Rev.*, 2022, **122**, 2292-2352.
- (a) D. A. DiRocco, K. Dykstra, S. Krska, P. Vachal, D. V. Conway and M. Tudge, *Angew. Chem., Int. Ed.*, 2014, **53**, 4802-4806; (b) T. Cernak, K. D. Dykstra, S. Tyagarajan, P. Vachal and S. W. Krska, *Chem. Soc. Rev.*, 2016, **45**, 546-576; (c) R. Budhwan, S. Yadav and S. Murarka, *Org. Biomol. Chem.*, 2019, **17**, 6326-6341; (d) S. K. Parida, S. K. Hota, R. Kumar and S. Murarka, *Chem. – Asian J.*, 2021, **16**, 879-889.
- S. R. Neufeldt and M. S. Sanford, *Adv. Synth. Catal.*, 2012, **354**, 3517-3522.
- M. Tobisu, T. Furukawa and N. Chatani, *Chem. Lett.*, 2013, **42**, 1203-1205.
- D. Li, C. Liang, Z. Jiang, J. Zhang, W.-T. Zhuo, F.-Y. Zou, W.-P. Wang, G.-L. Gao and J. Song, *J. Org. Chem.*, 2020, **85**, 2733-2742.
- R. K. Samanta, P. Meher and S. Murarka, *J. Org. Chem.*, 2022, **87**, 10947-10957.
- T. Sahoo, S. Banik, D. Vijaya Prasanna, B. Sridhar and B. V. Subba Reddy, *ChemPhotoChem*, 2024, **8**, e202400233.
- D. L. Golden, S.-E. Suh and S. S. Stahl, *Nature Reviews Chemistry*, 2022, **6**, 405-427.
- N. K. Mishra, S. Sharma, J. Park, S. Han and I. S. Kim, *ACS Catal.*, 2017, **7**, 2821-2847.
- A. Baralle, L. Fensterbank, J.-P. Goddard and C. Ollivier, *Chem. – Eur. J.*, 2013, **19**, 10809-10813.
- S. Senapati, S. K. Parida, S. S. Karandikar and S. Murarka, *Org. Lett.*, 2023, **25**, 7900-7905.
- M. A. T. Blaskovich, *J. Med. Chem.*, 2016, **59**, 10807-10836.

23. (a) L. F. Weigel, C. Nitsche, D. Graf, R. Bartenschlager and C. D. Klein, *J. Med. Chem.*, 2015, **58**, 7719-7733; (b) J. K. Stille, J. Tjuttrins, G. Wang, F. A. Venegas, C. Hennecker, A. M. Rueda, I. Sharon, N. Blaine, C. E. Miron, S. Pinus, A. Labarre, J. Plescia, M. Burai Patrascu, X. Zhang, A. S. Wahba, D. Vlaho, M. J. Huot, T. M. Schmeing, A. K. Mittermaier and N. Moitessier, *Eur. J. Med. Chem.*, 2022, **229**, 114046.
24. P. Meher, M. S. Prasad, K. R. Thombare and S. Murarka, *ACS Catal.*, 2024, **14**, 18896-18906.
25. C. Cavedon, P. H. Seeberger and B. Pieber, *Eur. J. Org. Chem.*, 2020, **2020**, 1379-1392.
26. A. F. Fearnley, J. An, M. Jackson, P. Lindovska and R. M. Denton, *Chem. Commun.*, 2016, **52**, 4987-4990.
27. H. Jiang, Y. Cheng, R. Wang, Y. Zhang and S. Yu, *Chem. Commun.*, 2014, **50**, 6164-6167.
28. Y. Chen, C. Shu, F. Luo, X. Xiao and G. Zhu, *Chem. Commun.*, 2018, **54**, 5373-5376.
29. S. Mkrtchyan and V. O. Iaroshenko, *Chem. Commun.*, 2020, **56**, 2606-2609.
30. P. Meher, R. K. Samanta, S. Manna and S. Murarka, *Chem. Commun.*, 2023, **59**, 6092-6095.
31. K. R. Thombare, S. K. Parida, P. Meher and S. Murarka, *Chem. Commun.*, 2024, **60**, 13907-13910.
32. J. Franck and E. Rabinowitsch, *Trans. Faraday Soc.*, 1934, **30**, 120-130.
33. T. Sahoo, D. V. Prasanna, B. Sridhar and B. V. Subba Reddy, *Org. Biomol. Chem.*, 2024, **22**, 9408-9412.
34. W. Lecroq, P. Bazille, F. Morlet-Savary, M. Breugst, J. Lalevée, A.-C. Gaumont and S. Lakhdar, *Org. Lett.*, 2018, **20**, 4164-4167.
35. D. I. Bugaenko, A. A. Volkov, M. V. Livantsov, M. A. Yurovskaya and A. V. Karchava, *Chem. – Eur. J.*, 2019, **25**, 12502-12506.
36. P. Meher, S. K. Parida, S. K. Mahapatra, L. Roy and S. Murarka, *Chem. – Eur. J.*, 2024, **30**, e202402969.
37. J. Galicia, N. R. McDonald, C. W. Bennett, J. He, M. D. Glossbrenner and E. A. Romero, *Chem. Commun.*, 2024, **60**, 6929-6932.
38. T.-Y. Ding, X.-N. Guo, B. Chen, C.-H. Tung and L.-Z. Wu, *Adv. Synth. Catal.*, 2025, **367**, e202401240.
39. Y. Wang, L. Wang and J. Han, *Org. Lett.*, 2025, **27**, 1012-1017.
40. N.-W. Liu, S. Liang and G. Manolikakes, *Adv. Synth. Catal.*, 2017, **359**, 1308-1319.
41. A. M. Nair, S. Kumar, I. Halder and C. M. R. Volla, *Org. Biomol. Chem.*, 2019, **17**, 5897-5901.
42. C. Breton-Patient, D. Naud-Martin, F. Mahuteau-Betzer and S. Piguel, *Eur. J. Org. Chem.*, 2020, **2020**, 6653-6660.
43. S. Zhang, Q. Zhang, S. Lin, X. Lin and X. Huang, *RSC Adv.*, 2024, **14**, 14697-14701.
44. D. Sun, K. Yin and R. Zhang, *Chem. Commun.*, 2018, **54**, 1335-1338.
45. Z. Chen, N.-W. Liu, M. Bolte, H. Ren and G. Manolikakes, *Green Chem.*, 2018, **20**, 3059-3070.
46. N.-W. Liu, Z. Chen, A. Herbert, H. Ren and G. Manolikakes, *Eur. J. Org. Chem.*, 2018, **2018**, 5725-5734.
47. A. M. Nair, I. Halder, S. Khan and C. M. R. Volla, *Adv. Synth. Catal.*, 2020, **362**, 224-229.
48. G. Fumagalli, S. Boyd and M. F. Greaney, *Org. Lett.*, 2013, **15**, 4398-4401.
49. M. N. Hopkinson, B. Sahoo and F. Glorius, *Adv. Synth. Catal.*, 2014, **356**, 2794-2800.
50. A. Bunescu, Y. Abdelhamid and M. J. Gaunt, *Nature*, 2021, **598**, 597-603.
51. B. Li, A. Bunescu and M. J. Gaunt, *Chem*, 2023, **9**, 216-226.
52. B. Li, A. Bunescu, D. Drazen, K. Rolph, J. Michalland and M. J. Gaunt, *Angew. Chem., Int. Ed.*, 2024, **63**, e202405939.
53. L. Capaldo, D. Ravelli and M. Fagnoni, *Chem. Rev.*, 2022, **122**, 1875-1924.
54. B. Ye, J. Zhao, K. Zhao, J. M. McKenna and F. D. Toste, *J. Am. Chem. Soc.*, 2018, **140**, 8350-8356.
55. X. Xie, K. Qiao, B.-r. Shao, W. Jiang and L. Shi, *Org. Lett.*, 2023, **25**, 4264-4269.
56. H. Wang, H. Jiang, S. Lin, S. Zhang and X. Huang, *Adv. Synth. Catal.*, 2024, **366**, 4765-4771.
57. (a) X.-Y. Lv and R. Martin, *Org. Lett.*, 2023, **25**, 3750-3754; (b) X. Zeng, C. Wang, W. Yan, J. Rong, Y. Song, Z. Xiao, A. Cai, S. H. Liang and W. Liu, *ACS Catal.*, 2023, **13**, 2761-2770; (c) W. Yan, A. T. Poore, L. Yin, S. Carter, Y.-S. Ho, C. Wang, S. C. Yachuw, Y.-H. Cheng, J. A. Krause, M.-J. Cheng, S. Zhang, S. Tian and W. Liu, *J. Am. Chem. Soc.*, 2024, **146**, 15176-15185.
58. L. Caiger, H. Zhao, T. Constantin, J. J. Douglas and D. Leonori, *ACS Catal.*, 2023, **13**, 4985-4991.

View Article Online
DOI: 10.1039/D5CC02800K

No primary research results, software or code have been included and no new data were generated or analysed as part of this review.